JAERI-M
4890

Numerical Analysis of the Magnetohydrodynamic Instabilities of Cylindrical and Toroidal Plasmas by the Finite Element Method

July 1972

Tatsuoki TAKEDA, Yasuo SHIMOMURA,
Mitsuru OHTA, Masaji YOSHIKAWA

日本原子力研究所
Japan Atomic Energy Research Institute

JAERI - M 4890

Numerical Analysis of the Magnetohydrodynamic Instabilities in Cylindrical and Toroidal Plasmas by the Finite Element Method

Tatsuoki TAKEDA, Yasuo SHIMOMURA,
Mitsuru OHTA and Masaji YOSHIKAWA
Nuclear Fusion Lab., Tokai, JAERI

(Received June 26, 1972)

A finite element method is proposed for stability analysis of a cylindrical current-carrying plasma embedded in a strong longitudinal magnetic field. These results of numerical analyses will be published in separate papers. The purpose of the present report, which supplements and is in considerable duplication with the subsequent papers, is twofold. That is, all the results obtained thus far are summarized, including also those which are not in the papers to be compact. The procedures of analyses are then given both in detail and comprehensively, to serve as a manual for users of the computer program. Furthermore the formulation is described for another computer program being prepared at present for stability analysis of toroidal current-carrying plasmas in general.

JAERI−M 4890

円筒プラズマおよびトロイダルプラズマの磁気流体不安定性の有限要素法による数値解析

日本原子力研究所東海研究所核融合研究室
竹田辰興・下村安夫・太田　充
吉川允二

（１９７２年６月２６日受理）

強い縦磁場中に置かれた，電流のある円筒プラズマの安定解析に，有限要素法を応用する事が提案された。数値解析の結果は別論文にて発表される。本報告書はこれらの論文を補足するものでまた重複する個所もあるが，その目的は次の通りである。第一に，本報告書は，新しい結果，および論文を簡潔にする為省かれた内容等をも含めて，今まで得られた全ての結果を包括するものである。第二には，計算機プログラムを使用する人にとって，本報告書がマニュアルの役目を果すように，解析の方法が詳細に且つ包括的に述べられている。更に，一般のトロイダルプラズマの安全性を解析する為に現在準備中の新しい計算機プログラムの定式化が述べられている。

CONTENTS

1. Introduction

The brilliant results obtained in tokamak experiments have renewed an interest in the study of magnetohydrodynamic stability in a current-darrying plasma. The problem have been studied extensively by many authors for some time. In particular the stability problems of the plasma in a cylindrical geometry have been solved analytically for various cases. For example, Tayler[1] obtained the growth rate explicitly by solving directly the equation of motion of the magnetohydrodynamic fluid. It is, however, sufficient to analyze the energy principle of Bernstein et al.[2] to obtain the stability criteria of the magneto-hydrodynamic fluid (a variational method). Analysis based on the principle has been carried out for a cylindrical plasma by, for example, Suydam[3]. Newcomb[4] has applied the variational method to more general cases and demonstrated a general procedure to give the stability criteria of diffuse linear pinches. On the other hand, Shafranov[5] has derived, explicitly, the stability criteria and gave the growth rate of instabilities in a current-carrying plasma embedded in a strong longitudinal magnetic field. These kind of approach are, however, applied only to special one-dimensional cases. The analytical methods are difficult to apply to a plasma with complicated geometry and complicated distribution of current and pressure. Even for axi-symmetric toroidal plasmas, there are no explicit solutions of general criteria of magnetohydrodynamic stability. As for the numerical analysis of the magnetohydrodynamic stability, the cylindrical plasma has been studied extensively by many authors[6,7]. Some authors[8-10] have successfully solved the stability problems of plasmas with more complicated geometry by integrating directly the time dependent magnetohydrodynamic equation. Excepting the above works, the numerical analysis so far are usually applied only to the one-dimensional problems because of the complexity of the numerical formulation. Nevertheless, the stability analysis of the plasmas of complicated geometry becomes more and more necessary, since several advantages of the shaped tokamaks are recently recognized.

We have proposed that the finite element method[11-13] can be applied to the analysis of the magnetohydrodynamic stabilities and showed that the numerical method could be successfully applied to the stability analysis of a cylindrical plasma[14,15]. In this article the method and results of the numerical investigation of the stability of a cylindrical current-carrying plasma are presented more comprehensively than in References 14 and 15, including results hitherto unpublished. The manual

of the computer program for the analysis of a cylindrical plasma is presented for the users of the program.

Comparing with an analytical approach, the stability analysis of a plasma with complicated geometry is carried out by the finite element method without any analytical approximation, such as an expansion by a small parameter. A computer program for stability analysis of general toroidal plasma is now under preparation. The formulation of the program is also presented.

Section 2 describes the method of the numerical calculation. In Sec. 3 the numerical results of the stability analysis of the cylindrical current-carrying plasma with a strong longitudinal magnetic field are shown and compared with the analytical ones. In Sec. 4 we discuss the results as well as the stability, convergence and accuracy of the numerical calculation.

2. Method of the calculation

(2-1) Basic equations

The finite element method is one of the computational methods based on the variational principle, which has been intensively developed in the field of the structural analysis[11-13]. We consider a system where a Lagrangian is defined. In the following discussions we restrict ourselves to the case where the Lagrangian is represented as an integral of the quadratic form of the variables and their time derivatives. In the stability analysis the energy integral of Bernstein et al.[2] minus the kinetic energy is taken as the Lagrangian which satisfies the above conditions, where the variables are the displacement vector of the plasma ($\boldsymbol{\xi}$) and the perturbed vector potential in the vacuum ($\mathbf{A}$). The potential energy (W) consists of three parts, that is,

$$W = W_p + W_s + W_v \tag{1}$$

where W_p, W_s and W_v are the potential energies of the plasma, the plasma-vacuum surface and the vacuum, respectively, which are given by

$$W_p = \frac{1}{2}\int d\tau \left\{ |\mathbf{Q}|^2 - \mathbf{j}\cdot\mathbf{Q}\times\boldsymbol{\xi} + \gamma P (\mathrm{div}\,\boldsymbol{\xi})^2 + (\mathrm{div}\,\boldsymbol{\xi})(\boldsymbol{\xi}\,\mathrm{grad}\,P) \right\} , \tag{2}$$

$$W_s = \frac{1}{2}\int d\sigma\, (\mathbf{n}\cdot\boldsymbol{\xi})^2 \left\langle \mathrm{grad}\left| P + \frac{1}{2}|\mathbf{B}|^2 \right| \right\rangle , \tag{3}$$

$$W_v = \frac{1}{2}\int d\tau\, |\mathrm{rot}\,\mathbf{A}|^2 , \tag{4}$$

where $\mathbf{Q} = \mathrm{rot}(\boldsymbol{\xi}\times\mathbf{B})$, $\mathbf{n}$ is the unit normal vector of the plasma-vacuum surface, $\mathbf{j}$, $\mathbf{B}$ and P are the current density, the magnetic flux density and plasma pressure in the equilibrium state, respectively, γ is the ratio of the specific heat of the plasma, $d\tau$ and $d\sigma$ are a volume element and a surface element, respectively and $\langle X \rangle$ denotes the increment of a quantity X across the surface in the direction $\mathbf{n}$. When we assume that the displacement varies in time as $\exp(i\omega t)$, the kinetic energy is given by

$$\omega^2 K = \frac{1}{2}\omega^2 \int d\tau\, \rho_p \left(\xi_r^2 + \xi_\theta^2 + \xi_z^2 \right), \tag{5}$$

where ρ_p is the plasma density. After dividing the region into a number of meshes and defining the functional form of dependence of the variables on the position inside each mesh, the Lagrangian is represented by a

quadratic form of the values of variables at the mesh points. Therefore from the variation of the Lagrangian, the stability problem of the system is reduced to an eigenvalue problem of a matrix, which is related to the potential and the kinetic energies in the form of

$$\left| C - \omega^2 R \right| = 0 \quad , \tag{6}$$

where C and R are the matrices relating to the potential and the kinetic energies, respectively. To determine whether the system is stable or not, it is sufficient to see if there are any negative eigenvalues of the above characteristic equation. If there is at least one negative eigenvalue ($\omega^2 < 0$), then from the minimum eigenvalue (ω_{min}^2) we find the growth rate of the most unstable mode as

$$\Gamma = (-\omega_{min}^2)^{\frac{1}{2}} \quad . \tag{7}$$

(2-2) Derivation of the characteristic equation determining the growth rate of instability

In this subsection in order to simplify the formulation we describe only the case of the one-dimensional (cylindrical) current-carrying plasma embedded in a strong longitudinal magnetic field. The formulation of the stability analysis of a general axi-symmetric toroidal plasma is given in Appendix C. The plasma is encased in a conducting wall separated by a vacuum. Because of the symmetries along and around the z axis, the energy integral of the plasma [Eq. (2)] is reduced to the one-dimensional energy integral as

$$W_p = \frac{\pi}{2} \int r dr \Big\{ \Lambda \left(\xi , \frac{d\xi}{dr} \right) + \gamma P \left[\eta + \frac{1}{r} \frac{d}{dr} (r \xi) \right]^2 + \frac{k^2 r^2 + m^2}{r^2} \left[\zeta - \zeta_0 \left(\xi , \frac{d\xi}{dr} \right) \right]^2 \Big\}, \tag{8}$$

where

$$\Lambda \left(\xi , \frac{d\xi}{dr} \right) = \frac{r}{k^2 r^2 + m^2} \left[(k r B_z + m B_\theta) \frac{d\xi}{dr} + (k r B_z - m B_\theta) \frac{\xi}{r} \right]^2 + \left[(k r B_z + m B_\theta)^2 - 2 B_\theta \frac{d}{dr} (r B_\theta) \right] \frac{\xi^2}{r^2} \quad , \tag{9}$$

$$\zeta_0 \left(\xi , \frac{d\xi}{dr} \right) = \frac{r}{k^2 r^2 + m^2} \left[(k r B_\theta - m B_z) \frac{d\xi}{dr} - (k r B_\theta + m B_z) \frac{\xi}{r} \right], \tag{10}$$

$$\xi = \xi_r , \quad \eta = \frac{im}{r} \xi_\theta + ik \xi_z , \quad \zeta = i \xi_\theta B_z - i \xi_z B_\theta \quad , \tag{11}$$

ξ_r, ξ_θ and ξ_z are the components of the displacement vector in the cylindrical coordinate system, where it should be noted that ξ_r, $i\xi_\theta$ and $i\xi_z$ are real functions of r. The magnetic field $\mathbf{B}$ and the plasma pressure P are related to the plasma current $\mathbf{j}$ through the following relation,

$$\mathbf{j} = \mathrm{rot}\,\mathbf{B}\ , \tag{12}$$

$$P = \mathbf{j} \times \mathbf{B}\ . \tag{13}$$

The energy integral of the plasma-vacuum surface is reduced to

$$W_S = \frac{\pi}{2} a \xi_r^2(a) \left\langle \frac{d}{dr}\left(P + \frac{1}{2}|\mathbf{B}|^2\right)\right\rangle , \tag{14}$$

where a is the radius of the plasma.
The boundary conditions are

$$A_\theta = -\xi_r B_z,\ A_z = \xi_r B\ , \tag{15}$$

at the plasma-vacuum surface (r = a),

$$A_\theta = 0,\quad A_z = 0, \tag{16}$$

at the surface of the conducting wall (r = b).
When we consider a fixed boundary problem, that is, when the region inside the conducting wall is filled with the plasma, only the energy integral of the plasma (W_p) should be taken into account. In this case the boundary conditions are reduced to

$$\xi_r = 0\quad , \tag{17}$$

at the boundary.

For the formulation of the finite element method we should divide the whole region into a number of meshes, at first. For simplicity, the displacement vector $\xi(\mathbf{r})$ at the position $\mathbf{r}$ is assumed to be a linear function of the position which is determined by the vectors at the mesh points of the mesh which contains the position $\mathbf{r}$, that is,

$$\xi(\mathbf{r}) = \sum_i \varphi_i(\mathbf{r})\,\xi_i\ , \tag{18}$$

where ξ_i is the displacement vector at the i-th mesh point of the mesh

and $\varphi_i(\mathbf{r})$ is a linear function of $\mathbf{r}$. As we are now interested in the one-dimensional case, Eq. (18) is reduced to

$$\xi(r) = \frac{1}{r_{j+1}-r_j}\left[(r-r_j)\xi_{j+1} + (r_{j+1}-r)\xi_j\right], \qquad (18')$$

in the j-th mesh, where we denote the region $[r_j, r_{j+1}]$ as the j-th mesh. Throughout the calculations, we divide the region into meshes with equal width except the cases where we investigate the convergence of the numerical calculation (see Sec. 4). Then substituting $\xi(r)$ in the form of Eq. (18') into the Lagrangian, the Lagrangian is reduced to a quadratic form of the components of the displacement vectors at the mesh points as

$$L = W - \omega^2 K , \qquad (19)$$

where

$$W = (\tilde{\xi}, C\tilde{\xi}), \qquad (20)$$

and

$$K = (\tilde{\xi}, R\tilde{\xi}), \qquad (21)$$

L, W and $\omega^2 K$ are the Lagrangian, the potential energy and the kinetic energy of the system, respectively, N is the number of the mesh points and C and R are symmetric matrices. $\tilde{\xi}$ is defined as

$$\tilde{\xi} = {}^t({}^t\xi_1, {}^t\xi_2, \cdots\cdots {}^t\xi_N), \qquad (22)$$

where ${}^t\xi$ indicates a transposed vector of ξ. The explicit form of the matrices C and R for the one-dimensional case is given in Appendix A. If there is no constraining condition, C and R are the matrices of order 3N. Constraining conditions such as div $\xi = 0$ and the boundary condition reduce the order of the matrices.

When we solve a free boundary problem, it is convenient to represent the vacuum integral by the displacement vectors at the plasma-vacuum boundary. For the one-dimensional case it is carried out easily because the perturbed field in the vacuum region can be obtained analytically[1]. According to Ref. 1) and the boundary condition [Eq. (15)] the vacuum integral is derived as

$$W_V = \frac{\pi}{2}\int r\,dr\,(\delta B_r^2 + \delta B_\theta^2 + \delta B_z^2), \qquad (23)$$

$$\delta B_r^2 + \delta B_\theta^2 + \delta B_z^2 = \xi^2(a) \cdot \frac{B_\theta^2(a)}{k^2 a^2} \quad \frac{1}{\left[K_m'(ka) I_m'(kb) - I_m'(ka) K_m'(kb) \right]}$$

$$\times \left\{ k^2 \left[K_m'(kr) I_m'(kb) - I_m'(kr) K_m'(kb) \right]^2 + \left(\frac{m^2}{r^2} + k^2 \right) \right.$$

$$\left. \left[K_m'(kr) I_m'(kb) - I_m'(kr) K_m'(kb) \right]^2 \right\}, \qquad (24)$$

where δ indicates the perturbed quantities, and K_m and I_m are the modified Bessel functions. It should be noted that in the case of the multi-dimensional problems (e.g. an axi-symmetric toroidal plasma) the vacuum energy can not be represented in general as an analytical function of the displacement vectors at the plasma-vacuum boundary. Therefore the vacuum energy should be calculated numerically (Appendix B). Thus the potential energy of the whole system including the plasma, the surface and the vacuum is represented as a quadratic form of the components of the displacement vectors at the mesh points in the plasma. After substituting the potential energy and the kinetic energy thus obtained into the Lagrangian [Eq. (19)], the variation of the Lagrangian gives a characteristic equation [Eq. (6)]. Thus the stability problem of the plasma is reduced to an eigenvalue problem of a matrix.

(2-3) Computer codes for the stability analysis of a cylindrical plasma

Three kinds of computer codes were programed for the stability analysis of a cylindrical plasma. By Codes I, and II we can analyze the cases with two- and one- constraining conditions, respectively. The case without any constraining condition can be calculated by Code III. By Code III, Eq.(6)is solved for the three variables ξ_r ξ_θ and ξ_z. In Code II, however, the variable ξ_θ is eliminated by assuming that the plasma is incompressible (div $\xi = 0$). Therefore the Lagrangian for Code II is a functional of the variables ξ_r and ξ_θ. In Code I an additional condition ($\xi = \xi_0$) is taken into account and the only one variable in Code I is ξ_r. In Codes III and II, Eq. (6) is solved by applying Jacobi's method twice to the eigenvalue problems of the matrix as seen later. Code I is, however, programmed for saving computational time and the eigenvalue problem of the matrix is solved numerically only once. The computational time of Code I is less than that of Code III by about a factor of six. In the following we describe Codes III and I in some detail.

As the matrix R in Eq. (6) is not a unit matrix we solve the equation by transforming the matrix R into a unit matrix E as

$$|C'' - \omega^2 E| = 0 \quad , \tag{25}$$

where

$$C'' = BC'B \quad , \tag{26}$$

$$C' = V_1^{-1} C V_1 \quad , \tag{27}$$

it should be noted that B is a diagonal matrix which satisfies a relation $B \cdot B = V_1^{-1} \cdot R \cdot V_1$ where V_1 is an orthogonal matrix. The matrix C" can be diagonalized by an orthogonal matrix V_2 as $V_2^{-1} C'' V_2$. The eigenvector corresponding to the i-th eigenvalue $\tilde{\xi}_i$ is given by the i-th row vector of a matrix $V_1 B V_2$.

As for Code I, we solve the following eigenvalue problem;

$$|C - \omega^2 E| = 0 \tag{28}$$

We use the eigenfunction $\tilde{\xi}'$ of Eq. (28) as trial functions of the variational method and obtain approximate eigenvalues of Eq. (6) as

$$\omega'^2 = \frac{(\tilde{\xi}', C\tilde{\xi}')}{(\tilde{\xi}', R\tilde{\xi}')} \quad . \tag{29}$$

It should be noticed that the sign of the eigenvalue ω'^2 is same as that of ω^2. Therefore the numerical results of Code I is valid at least, as long as the stability region is discussed. As for the growth rate of instability, it is accurate only within an order of magnitude.

The numerical calculations are carried out by using FACOM 230/60 electronic computer. The flow chart, the program list and the input data format of Code III are presented in Appendix D.

3. The results of the numerical calculation

We assume that there is no azimuthal plasma current j_θ which means that the longitudinal magnetic field B_z is uniform and that the dependence of the longitudinal plasma current j_z on the radius r is given in the form

$$j_z(r) = j_0 + j_1(1-r^s) + j_2 r(1-r^t), \tag{30}$$

where the second term corresponds to the variation of the current distribution from the flat to the one concentrated near the plasma axis and the third term represents a skin current. The longitudinal wave number k (= $2\pi n/L$) is taken to be $0.2/a$ throughout the calculation, where n and L are the longitudinal mode number and the periodic length of the plasma, respectively, and the plasma radius a is normalized to unity.

At first we briefly describe the results of numerical calculation of the fixed boundary problems[14]. To compare with the analytical results[5] we studied the case of an incompressible plasma with a uniform current density ($j_1 = j_2 = 0$). Shafranov[5] has given the growth rate of the instability for the system as[15]

$$\Gamma^2 = \frac{B_\theta^2(a)}{4\pi\rho_p a^2}\left[2|m-nq_a|\frac{2\pi na}{L\cdot Z_m} - (m-nq_a)^2\right], \tag{31}$$

where $q_a = \dfrac{2\pi a B_z(a)}{L B_\theta(a)}$ is the safety factor and Z_m is the zero of the Bessel function $J_m(Z)$. Figure 1 illustrates the growth rate given by Eq. (31) as well as the growth rate obtained by the numerical analysis. The numerical result is in good agreement with the analytical one. A part of the small difference between the numerical and the analytical results is explained by the fact that the analytical results is obtained under the assumption $k^2a^2 \ll 1$. In the fixed boundary problem the growth rate of instability depends very much on the specific heat of the plasma. When the plasma is compressible, a double peak of the growth rate as shown in Fig. 1 degenerates into a single peak gradually as γ is decreased and the growth rate becomes larger (Fig. 2). The growth rate of the $\gamma = 5/3$ plasma is larger than that of the incompressible one by about a factor of 3. It is also shown in Fig. 2 that the growth rate is smaller for higher m-mode if k is kept constant.

Next, we shall describe the results of the calculations of the free boundary case. The dependence of the growth rate on the current distribution (Fig. 3) is shown for the case of $\gamma = 5/3$. The growth rates of instability for various current distributions are illustrated in Figs. 4

and 5. It is found from Fig. 5 that for modes with m=2 a plasma with the current distributions concentrated near the axis is more stable than a plasma with a flatter or skin-like current distribution. It is in agreement with the qualitative results given in reference 5). On the other hand, the growth rate of the m=1 mode is independent of the current distribution and the unstable region for the mode is given by

$$\left(\frac{a}{b}\right)^2 \lesssim nq_a \lesssim 1 \qquad (32)$$

which is also predicted analytically[5]. To summarize the dependence of growth rates on the current distribution, the unstable regions in the nq_a-1/s plane are illustrated in Fig. 6. In this figure the unstable regions are bounded by the vertical lines and the curves to the left. The diagram is obtained by minimizing the potential energy integral (W) which is a functional of only the radial component of displacement vectors ξ_r, for saving the computational time (Code-I). The effect of compressibility was also investigated by comparing the cases for $\gamma = 5/3$, $5/3 \times 500$, $5/3 \times 1000$ and $5/3 \times 5000$. In contrast with the fixed boundary case, the growth rate hardly depends on the ratio of specific heat. An example of the dependence of the growth rate on the ratio is shown in Fig. 7.

The stabilizing effect of a conducting wall placed near the plasma is shown in Figs. 7 and 8. The figures show the dependence of the growth rate on the wall position (b/a) for the m=2 and m=1 modes, respectively. It is concluded that the conducting wall is not effective for the stabilization of the m=2 and m=3 modes, if the radius of the conducting wall is larger than twice the plasma radius ($b \geq 2a$). The conducting wall is very effective to stabilize these modes, if the radius of the wall is less than twice the plasma radius ($b < 2a$). For higher m instabilities ($m \geq 4$), however, the conducting wall is less effective even if the radius of the wall is less than 2a. In case of nearly flat distribution (s = 20), unstable regions of the m=4 mode are $3.35 < nq_a < 4$ and $3.40 < nq_a < 4$ for b/a = 2.0 and b/a = 1.4, respectively. And the maximum growth rate is the same for both case within 10 %.

The effect of such a variation of the logitudinal field across the plasma is studied by using the computer code. Figure 9 shows the growth rates when the longitudinal field in the plasma is varied slightly from the field in the vacuum. Here the radial distribution of the longitudinal field is assumed to be in the form of

$$B_t(r) = B_t(a)\cdot\left[\,1 - D\,(r^2-1)^2\,\right]. \qquad (33)$$

Since in the tokamak experiment it is found that the longitudinal magnetic field in the plasma changes at most by 0.01 % from the vacuum field, such a small change of the longitudinal magnetic field should have a negligible effect on the stability of the plasma.

4. Discussion

In the previous section we described the results of the numerical calculations for a cylindrical current-carrying plasma in a strong longitudinal magnetic field. Roughly speaking, they are in good agreement with the analytical results. For example, some of the analytical results obtained approximately are confirmed by the numerical calculations. There are, however, some discrepancies between the numerical results and the analytical ones. Some of them may be inherent in the numerical method.

As stated in Sec. 2, most calculations were made for the systems of meshes with equal width. In some cases a better result is obtained by a system of meshes which are chosen more carefully. For example, we first divide the plasma radius into N_0 meshes with the equal width of $h = a/N_0$ and then subdivide the mesh nearest to the plasma boundary into N_1 submeshes according to a geometrical progression of ratio 2 toward the boundary, that is, the width of the smallest mesh is $2^{-N_1} h$. Figures 4 and 10 show the dependence of the growth rate on N_0 and N_1 for the equilibrium configuration of a very concentrated current distribution with s=2. It is seen that the growth rate converges more rapidly by the subdivision described above in the region where the displacement is expected to change rapidly. It is also found that the convergence of the numerical calculation depends greatly on the distribution of the equilibrium quantities assumed. For example, better convergence was attained in case of a flatter current distribution.

In summary it is concluded that the finite element method can be successfully applied to the stability analysis of megnetohydrodynamic stability of the cylindrical plasma. There are, however, a number of questions to be answered, which are concerned with the convergence and the accuracy of the numerical calculation. These questions are more complicated when the finite element method is applied to a toroidal plasma, because a wide variety of selection of meshes is possible in the toroidal case. Nevertheless, it can be safely said that the finite element method is promising for the analysis of the stabilities of the toroidal plasma with complex geometry because of the easiness of the formulation of the method in incorporating complex boundary condition. We are now in the process of setting up a larger computer program to be applied to the stability analysis of an axi-symmetric toroidal plasma with arbitrary cross-section (Appendix C).

ACKNOWLEDGMENT

The authors are indebted to Dr. Masatoshi Tanaka and Mr. Takasi Tuda for their stimulating discussions and valuable suggestions. They wish to express their sincere thanks to Drs. Satoshi Itoh and Sigeru Mori for their discussions and encouragement.

Appendix A Explicit quadratic forms of W and K in the plasma for one-dimensional case

The potential energy (W) and the kinetic energy (ω^2 K) of the whole system are represented by

$$W = \sum_{i=1}^{N} W_i \quad , \tag{A1}$$

$$\omega^2 K = \sum_{i=1}^{N} \omega^2 K_i \quad , \tag{A2}$$

where W_i and $\omega^2 K_i$ are the potential energy and the kinetic energy in the i-th mesh, respectively. In the i-th mesh the displacement vectors are represented by a linear function of the position as

$$\xi_\mu = \frac{1}{h} (x\xi_{\mu i} - y\xi_{\mu i+1}) \qquad (\mu = r, \theta \text{ and } z) \quad , \tag{A3}$$

where $x \equiv r_{i+1} - r$, $y \equiv r_i - r$ and $h \equiv r_{i+1} - r_i$. The integrands in the expression of the potential energy [Eq. (8)] and the kinetic energy [Eq. (5)] are then represented by the quadratic form of $\hat{\xi}_p$'s as

$$I = \sum_{p=1}^{6} \sum_{q=1}^{6} \alpha_{pq} \hat{\xi}_p \hat{\xi}_q \quad , \tag{A4}$$

where $\hat{\xi}_1 = \xi_r$, $\hat{\xi}_2 = \xi_\theta$, $\hat{\xi}_3 = \xi_z$, $\hat{\xi}_4 = \frac{d\xi_r}{dr}$, $\hat{\xi}_5 = \frac{d\xi_\theta}{dr}$ and $\hat{\xi}_6 = \frac{d\xi_z}{dr}$.
Therefore, after the integration is performed, the potential energy and the kinetic energy in the i-th element are given by quadratic forms of the components of the displacement vectors at the mesh points as

$$W_i = (\tilde{\xi}_i, C_i \tilde{\xi}_i) \quad , \tag{A5}$$

$$\omega^2 K_i = \omega^2 (\tilde{\xi}_i, R_i \tilde{\xi}_i) \quad , \tag{A6}$$

where ${}^t\tilde{\xi}_i = (\xi_{ri}, \xi_{\theta i}, \xi_{zi}, \xi_{ri+1}, \xi_{\theta i+1}, \xi_{zi+1})$. C_i and R_i are given by;

$$(C_i)_{\alpha\beta} = \frac{\pi}{2} \int_{r_i}^{r_{i+1}} dr (\tilde{C}_i)_{\alpha\beta} \quad . \tag{A7}$$

$$(R_i)_{\alpha\beta} = \frac{\pi}{2} \int_{r_i}^{r_{i+1}} dr (\tilde{R}_i)_{\alpha\beta} \quad . \tag{A8}$$

The expression of the matrices $\tilde{C}_i$ and $\tilde{R}_i$ is shown in Tables 1 and 2.

Appendix B Numerical derivation of the vacuum energy

At first, we divide the vacuum region (a, b) into M meshes. Then in the same way as shown in Appendix A for the plasma energy the vacuum energy is represented by a quadratic form of the components of the perturbed vector potentials (A) at the mesh points as

$$W_v = \frac{\pi}{2}\int_a^b \mathrm{rot}A\ ^2\ \mathrm{r\,dr} = (\alpha\ , H\alpha) \quad , \tag{B1}$$

where ${}^t\alpha = (A_{\theta 1},\ A_{Z1},\ A_{r1},\ A_{r2},\ A_{\theta 2},\ A_{Z2}\ \cdots\cdots\ A_{rM+1})$, it should be noted that we have changed the order of the first three components $(A_{r1},\ A_{\theta 1},\ A_{Z1})$ because of the convenience in the expression as we shall see below and that we have dropped $A_{\theta M+1}$ and A_{ZM+1} because they are equal to zero.

The matrix H is made of smaller matrices H_i which is given by

$$(H_i)_{\alpha\beta} = \frac{\pi}{2}\int_{r_i}^{r_{i+1}} dr\,(\widetilde{H}_i)_{\alpha\beta} \quad . \tag{B2}$$

The expression of the matrices $\widetilde{H}_i$ is shown in Table 3. If $A_{\theta 1}$ and A_{Z1} are known, the extremum of W_V is given by differentiating W_V with respect to A_{r1}, A_{r2}, $A_{\theta 2}$, ... , and A_{rM+1}, and solving the linear simultaneous equation thus obtained. By substituting the solution into Eq. (B1), the vacuum energy is derived as a function of $\xi_r(a)$ using the boundary condition [Eq. (15)].

We shall describe below the above-mentioned procedure in more detail. We define the following matrices

$$\mathfrak{A}_{11} = \begin{pmatrix} H_{11} & H_{12} \\ H_{21} & H_{22} \end{pmatrix} \tag{B3}$$

$$\mathfrak{A}_{22} = \begin{pmatrix} H_{33} & H_{34} \cdots\cdots\cdots\cdots & H_{3n} \\ & \cdots\cdots\cdots\cdots & \\ & \cdots\cdots\cdots\cdots & \\ H_{n3} & H_{n4} \cdots\cdots\cdots\cdots & H_{nn} \end{pmatrix} \quad , \tag{B4}$$

$$\mathfrak{A}_{21} = \mathfrak{A}_{12} = \begin{pmatrix} H_{31} & H_{32} \\ \cdots\cdots & \\ \cdots\cdots & \\ H_{n1} & H_{n2} \end{pmatrix} \quad , \tag{B5}$$

where H_{ij}'s are the elements of the matrix H and n = 3M+1. The linear simultaneous equation, the roots of which determine the extremum state of the vacuum energy is obtained as

$$\mathfrak{A}_{22}\alpha' = -\mathfrak{A}_{21}\hat{\alpha}' \ , \tag{B6}$$

where $\alpha' = {}^t(A_{r1}, A_{r2}, A_{\theta 2} \cdots\cdots\cdots A_{rM+1})$ and $\hat{\alpha} = {}^t(A_{\theta 1}, A_{Z1})$. From this equation α is derived as

$${}^t\alpha = \mathfrak{A}\hat{\alpha} \ , \tag{B7}$$

where $\mathfrak{A} = \begin{pmatrix} 1 & 0 \\ 0 & 1 \\ -(\mathfrak{A}_{22}^{-1}\ \mathfrak{A}_{21}) & \end{pmatrix}$.

Therefore, the vacuum energy is represented by $A_{\theta 1}$ and A_{Z1} as

$$W_v = (\hat{\alpha}, \hat{H}\ \hat{\alpha}) \ , \tag{B8}$$

where $\hat{H} = {}^t\mathfrak{A} H \mathfrak{A}$ is a 2 × 2 matrix. Using the boundary condition at the plasma-vacuum boundary [Eq. (15)] the vacuum energy is represented by the radial component of the displacement vector at the boundary as

$$W_v = (B_z^2(a)\hat{H}_{11} - 2B_z(a)\ B_\theta(a)\hat{H}_{12} + B_\theta^2(a)\hat{H}_{22})\,\xi_r^2(a) \ . \tag{B9}$$

Appendix C Application of the finite element method to the stability analysis of an axi-symmetric toroidal plasma

As we are concerned with an axisymmetric toroidal plasma it is covenient to choose a cylindrical co-ordinate system R, ϕ and Z which is illustrated in Fig. 11. We assume that the magnetic axis is located at $R = R_0$ and $Z = 0$ and define Ψ as the magnetic flux threaded the short way around this axis per radian in ϕ. We also choose a locally orthogonal set of co-ordinate Ψ, χ and ϕ on a flux surface Ψ so that line elements are defined by

$$dx_\psi = \frac{d\psi}{RB_\chi} , \qquad dx_\chi = J B_\chi d\chi , \quad dx_\varphi = R d\varphi , \tag{C1}$$

where J is the Jacobian of the transformation.

From Eqs. (12 and 13), an equation of the equilibrium state is derived and is represented in this co-ordinate system as;

$$R \frac{d}{\partial R} \left(\frac{1}{R} \frac{\partial \psi}{\partial R}\right) + \frac{\partial^2 \psi}{\partial z^2} = R j_\varphi = - II' - R^2 P' , \tag{C2}$$

where

$$P = P(\psi) , \qquad I = I(\psi) = RB_\varphi , \tag{C3}$$

the other quantities are functions of χ and Ψ and a prime denotes differentiation with respect to Ψ. Using these relations, the three parts of the potential energy and the kinetic energy defined by Eqs. (2~5) can be, respectively, rewritten as;

$$\begin{aligned} W_p = \frac{1}{2} \int J d\psi d\chi d\varphi \Bigg[& \frac{1}{R^2 J^2 B_\chi^2} \left| \frac{\partial X}{\partial \chi} + \mu \frac{\partial X}{\partial \varphi} \right|^2 + B_\chi^2 \left| \frac{\partial U}{\partial \varphi} + \frac{\partial X}{\partial \psi} \right|^2 + \frac{R^2}{J^2} \\ & \times \left| - \frac{\partial}{\partial \psi} \mu x + \frac{\partial U}{\partial X} \right|^2 + \frac{\gamma P}{J^2} \left| \frac{\partial}{\partial \psi} JX + \frac{\partial Z}{\partial \chi} + \mu \frac{\partial Z}{\partial \varphi} + J \frac{\partial U}{\partial \psi} \right|^2 + X P' \left| \frac{\partial}{\partial \psi} JX \right. \\ & + \frac{\partial Z}{\partial \chi} + \mu \frac{\partial Z}{\partial \varphi} + J \frac{\partial U}{\partial \varphi} \Big| + \frac{I'X}{J} \left(- \frac{\partial}{\partial \psi} \mu X + \frac{\partial U}{\partial \chi} \right) - \left(\frac{UI'}{J} + \frac{II'Z}{R^2 J} \right) \left(\frac{\partial X}{\partial \chi} + \mu \frac{\partial X}{\partial \varphi} \right) \\ & + \frac{j_\varphi Z}{RJ} \left(\frac{\partial X}{\partial \chi} + \mu \frac{\partial X}{\alpha \varphi} \right) - \frac{j_\varphi X}{R} \left(\frac{\partial U}{\partial \varphi} + \frac{\partial X}{\partial \varphi} \right) \Bigg] , \end{aligned} \tag{C4}$$

$$W_s = \frac{1}{2} \int_{\Psi = \Psi_s} J d\psi d\chi d\varphi \frac{\langle X \rangle^2}{RB_\chi} \left\langle RB_\chi \frac{\partial}{\partial \psi} \left\{ P + \frac{1}{2} \left(B_\chi^2 + \left(\frac{I}{R} \right)^2 \right) \right\} \right\rangle , \tag{C5}$$

$$W_v=\frac{1}{2}\int J\,d\psi\,d\chi\,d\varphi\left[\frac{1}{R^2J^2B_\chi^2}\left|\frac{\partial}{\partial\chi}RA_\varphi-\frac{\partial}{\partial\varphi}JB_\chi A_\chi\right|^2+B_\chi^2\left|\frac{\partial}{\partial\varphi}\frac{A_\psi}{RB_\chi}-\frac{\partial}{\partial\psi}RA_\varphi\right|^2\right.$$

$$\left.+\frac{R^2}{J^2}\left|\frac{\partial}{\partial\psi}JB_\chi A_\chi-\frac{\partial}{\partial\chi}\frac{A_\psi}{RB_\chi}\right|^2\right] \quad , \tag{C6}$$

$$K=\frac{1}{2}\int J\,d\psi\,d\chi\,d\varphi\;\rho\left[\frac{X^2}{R^2B^2}+R^2U^2+\left(\frac{I^2}{R^2}+B^2\right)Z^2+2IUZ\right] \quad , \tag{C7}$$

where X, U and Z are the independent variables expressible in the terms of plasma displacement (ξ_ψ, ξ_χ, ξ_φ) as

$$X=RB_\chi\xi_\psi \quad , \quad Z=\xi_\chi/B_Z \quad , \quad U=\xi_\varphi/R-IZ/R^2 \quad , \tag{C8}$$

and the local pitch μ of the magnetic line of force defined to be

$$\mu = \frac{JI}{R^2} \quad . \tag{C9}$$

In the case of a plane-symmetric configuration with respect to the median plane, we can find eight sets of variables for different modes given in Table 4 which are classified in view of symmetry considerations. Then, W_p can be written as

$$W_p=\frac{\pi}{2}\int J\,d\chi\,d\psi\;\sum_{p=1}^{9}\sum_{q=1}^{9}\beta_{pq}\hat{Y}_p,\hat{Y}_q \quad , \tag{C10}$$

where $\hat{Y}_1=X$, $\hat{Y}_2=U$, $\hat{Y}_3=Z$, $\hat{Y}_4=\frac{\partial X}{\partial\psi}$, $\hat{Y}_5=\frac{\partial U}{\partial\psi}$, $\hat{Y}_6=\frac{\partial Z}{\partial\psi}$, $\hat{Y}_7=\frac{\partial X}{\partial\chi}$, $\hat{Y}_8=\frac{\partial U}{\partial\chi}$, $\hat{Y}_9=\frac{\partial Z}{\partial\chi}$ and β_{pq} are shown in Table 5.

For the analysis of the axisymmetric toroidal plasma, the energy integrals are expressed by the quantities on the cross-section of plasma, the section is devided into N_0 triangles as illustrated in Fig. 12. In the N-th element, a variable vector y is written as

$$y=\alpha_i y_i+\alpha_j y_j+\alpha_k y_k \quad , \tag{C11}$$

where

$$\alpha_i=\alpha\{(\psi_i\chi_k-\psi_k\chi_j)+(\chi_j-\chi_k)\psi+(\psi_k-\psi_j)\chi\}, \tag{C12}$$

$$\alpha_j=\alpha\{(\psi_k\chi_i-\psi_i\chi_k)+(\chi_k-\chi_i)\psi+(\psi_i-\psi_k)\chi\}, \tag{C13}$$

$$\alpha_k=\alpha\{(\psi_i\chi_j-\psi_j\chi_i)+(\chi_i-\chi_j)\psi+(\psi_j-\psi_i)\chi\}, \tag{C14}$$

$$\alpha^{-1}=\begin{vmatrix} 1, \psi_i, \chi_i \\ 1, \psi_j, \chi_j \\ 1, \psi_k, \chi_k \end{vmatrix} = \psi_j\chi_k-\psi_k\chi_j+\psi_k\chi_i-\psi_i\chi_k+\psi_i\chi_j-\psi_j\chi_i \ , \tag{C15}$$

and suffices i, j and k indicate the mesh points belonging to the N-th element. Then W_p is represented by

$$W_p = \sum_{N=1}^{N_0} W_{PN} \ , \tag{C16}$$

where

$$W_{PN} = \frac{\pi}{2} \int J \, d\chi \, d\phi \, F_N \ , \tag{C17}$$

$$F_N = (y^N, a^N y^N), \tag{C18}$$

$$^t y^N = (X_i, U_i, Z_i, X_j, U_j, Z_j, X_k, U_k, Z_k) \tag{C19}$$

and a^N is the matrix given in Table 5. In the same way, the other integrands are also represented by quadratic forms of the components of the displacement vectors at the mesh points. Then, the stability problem of the axisymmetric toroidal plasma is also reduced to an eigenvalue problem of a matrix [Eq. (6)] as in the case of a cylindrical plasma.

Appendix D Flow chart, program list and input data format of Code III

D-1 Flow chart

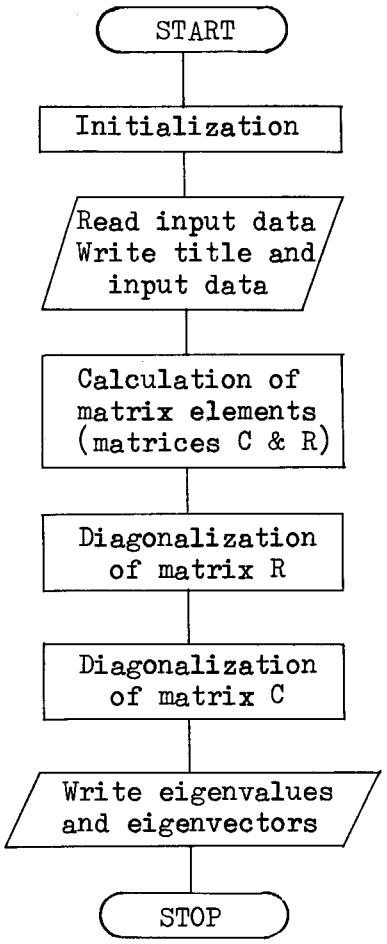

D-2. Program list of Code III (FORTRAN IV)

* SOURCE STATEMENT *

```
CCCCCCCCCCCCCCCCCCCCCCCCCCCCCCCCCCCCCCCCCCCCCCCCCCCCCCCCCCCCCCCCCCCCCCCCCCCCCC
C                                                                            C
C     STABILITY OF CYLDRICAL PLASMA BY F.E.M.                                C
C          THREE VAR.            FREE BOUNDARY                               C
C          1971  11                                                          C
C                                                                            C
CCCCCCCCCCCCCCCCCCCCCCCCCCCCCCCCCCCCCCCCCCCCCCCCCCCCCCCCCCCCCCCCCCCCCCCCCCCCCC
      COMMON/HEI/QA,ASP,A1,A2,A3,SS,SK,ST,DL                            MAIN  10
      COMMON/FX/SN,SM,RRHO                                              MAIN  20
      COMMON/XY/XYZ(50)                                                 MAIN  30
      COMMON/GGG/GAM                                                    MAIN  40
    1 FORMAT(F10.5,2I10)                                                MAIN  50
    2 FORMAT(4F10.5/7F10.5)                                             MAIN  60
    3 FORMAT(1H1,'     PLASMA RADIUS = 1.0 ,   WALL---B=',F12.5//       MAIN  70
     1'      N = ',I10,'      K= ',I10//                                MAIN  75
     2 '      RADIUS=H*(I-1)   H=1.0/N (I.LE.N-K)     H=H*0.5 (I.GT.N-K)'/)MAIN  80
    4 FORMAT(1H ,5X,'SN,SM,QA,ASP= ',4(3X,F12.5)/4X,'A1,A2,A3,SS,SK,ST= MAIN  90
     1',6(3X,F12.5)/4X,'DL=',3X,F12.5/4X,'RRHO= ',3X,F12.5/)            MAIN 100
    5 FORMAT(1H ,10X,'JZ =A1*(SS+2)/SS/ASP/QA*2*(1-R**SS)+A3*(ST+2)*(ST+MAIN 110
     23)/ASP/QA*R**ST*(1-R)'/)                                          MAIN 120
    6 FORMAT(1H ,3X,6HGAMMA=,1PE16.4//)                                 MAIN 130
    7 FORMAT(1H1)                                                       MAIN 140
      GAM=1.6667                                                        MAIN 150
      RRHO=0.001                                                        MAIN 160
      DO 23  I=1,50                                                     MAIN 170
      XYZ(I)=0.0                                                        MAIN 180
   23 CONTINUE                                                          MAIN 190
  200 READ(5,1) B,KZ,N                                                  MAIN 200
      IF(B.LT.1.0) GO TO 71                                             MAIN 210
      H=1./(N-KZ)                                                       MAIN 220
      WRITE(6,3) B,KZ,N                                                 MAIN 230
      WRITE(6,6) GAM                                                    MAIN 240
      READ(5,2) SN,SM,QA,ASP,A1,A2,A3,SS,SK,ST,DL                       MAIN 250
      WRITE(6,4)  SN,SM,QA,ASP,A1,A2,A3,SS,SK,ST,DL,RRHO                MAIN 260
      WRITE(6,5)                                                        MAIN 270
      CALL RHOX(B)                                                      MAIN 280
      WRITE(6,7)                                                        MAIN 290
      CALL MATRIX(H,N,KZ)                                               MAIN 300
      GO TO 200                                                         MAIN 310
   71 CONTINUE                                                          MAIN 320
      STOP                                                              MAIN 332
      END                                                               MAIN 340
```

```
      SUBROUTINE MATRIX(H,N,KZ)
      COMMON/XY/XYZ(50)
      DIMENSION C(50,50),V(50,50),RHO(70),PX1(50),PX2(50),PX3(50),
     1          CC(50,50),D(50,50),A(50,50),EIG(70),CJ(50,6,6),RJ(50,6,6)
      DOUBLE PRECISION A,E,RAM,EIG,EMIN,C,V,CC,D,RJ,RHO,CJ,ESP
   61 FORMAT(1H ,///'EIGEN VALUE  =',1PE12.4)
   70 FORMAT(1H ,3X,4HILL=,I10)                                        STAB 940
   75 FORMAT(1H ,///'          EIGEN VALUE   '/)
   80 FORMAT(1H ,10X,1P10E12.4)                                        STAB 886
   81 FORMAT(1H ,/'      EIGEN FUNCTION   R')
   82 FORMAT(1H ,/'      EIGEN FUNCTION   THETA')
   83 FORMAT(1H ,/'      EIGEN FUNCTION   Z')
   91 FORMAT(1H ,'   THETA      ',60X,'Z       '/)
   92 FORMAT(1H ,'   R'/)
      EPS=1.0D-14
      NJC=50
      N0=3*N                                                           STAB 160
      N1=3*N+3                                                         STAB 170
      DO 22 K=1,N1                                                     STAB 180
      DO 21 J=1,N1                                                     STAB 190
      C(J,K)=0.0                                                       STAB 200
   21 CONTINUE                                                         STAB 210
   22 CONTINUE                                                         STAB 220
      CALL CJRHO(CJ,RJ,H,N,KZ)
      C(1,1)=RJ(1,1,1)
      C(3,3)=RJ(1,3,3)
      C(1,2)=RJ(1,1,2)                                                 STAB 270
      C(2,2)=RJ(1,2,2)
      C(1,3)=RJ(1,1,3)
      C(2,3)=RJ(1,2,3)                                                 STAB 290
      C(N0+1,N0+1)=RJ(N,4,4)                                           STAB 300
      C(N0+2,N0+2)=RJ(N,5,5)                                           ST AB310
      C(N0+3,N0+3)=RJ(N,6,6)                                           STAB 320
      C(N0+1,N0+2)=RJ(N,4,5)                                           STAB 330
      C(N0+1,N0+3)=RJ(N,4,6)                                           STAB 340
      C(N0+2,N0+3)=RJ(N,5,6)                                           STAB 350
      DO131 J=1,N                                                      STAB 360
      J0=3*J                                                           STAB 370
      C(J0-2,J0+1)=RJ(J,4,1)                                           STAB 380
      C(J0-1,J0+1)=RJ(J,4,2)                                           STAB 390
      C(J0  ,J0+1)=RJ(J,4,3)                                           STAB 400
      C(J0-2,J0+2)=RJ(J,5,1)                                           STAB 410
      C(J0-1,J0+2)=RJ(J,5,2)                                           STAB 420
      C(J0  ,J0+2)=RJ(J,5,3)                                           STAB 430
      C(J0-2,J0+3)=RJ(J,6,1)                                           STAB 440
      C(J0-1,J0+3)=RJ(J,6,2)                                           STAB 450
      C(J0  ,J0+3)=RJ(J,6,3)                                           STAB 460
  131 CONTINUE                                                         STAB 470
      DO132 J=2,N                                                      STAB 480
      J0=3*J                                                           STAB 490
      C(J0-2,J0-2)=RJ(J,1,1)+RJ(J-1,4,4)                               STAB 500
      C(J0-1,J0-1)=RJ(J,2,2)+RJ(J-1,5,5)                               STAB 510
      C(J0  ,J0  )=RJ(J,3,3)+RJ(J-1,6,6)                               STAB 520
      C(J0-2,J0-1)=RJ(J,1,2)+RJ(J-1,4,5)                               STAB 530
      C(J0-2,J0  )=RJ(J,1,3)+RJ(J-1,4,6)

      C(J0-1,J0  )=RJ(J,2,3)+RJ(J-1,5,6)                               STAB 550
  132 CONTINUE                                                         STAB 560
      DO142 J=1,N1                                                     STAB 570
      DO141 K=1,J                                                      STAB 580
      C(J,K)=C(K,J)                                                    STAB 590
  141 CONTINUE                                                         STAB 600
  142 CONTINUE                                                         STAB 610
      CALL JACOBD(C,NJC,N1,EPS,V,ILL)
      WRITE(6,70) ILL                                                    20
      DO 300 K=1,N1                                                      30
      RHO(K)=C(K,K)
  300 CONTINUE                                                           50
      DO 504 I=1,N1
      DO 505 J=1,N1
      C(I,J)=0.0
      D(I,J)=V(I,J)                                                    STAB
  505 CONTINUE
  504 CONTINUE
      C(1,1)=CJ(1,1,1)                                                 STAB 240
      C(2,2)=CJ(1,2,2)                                                 STAB 250
      C(3,3)=CJ(1,3,3)                                                 STAB 260
      C(1,2)=CJ(1,1,2)                                                 STAB 270
      C(1,3)=CJ(1,1,3)                                                 STAB 280
      C(2,3)=CJ(1,2,3)                                                 STAB 290
      C(N0+1,N0+1)=CJ(N,4,4)                                           STAB 300
      C(N0+2,N0+2)=CJ(N,5,5)                                           ST AB310
      C(N0+3,N0+3)=CJ(N,6,6)                                           STAB 320
      C(N0+1,N0+2)=CJ(N,4,5)                                           STAB 330
      C(N0+1,N0+3)=CJ(N,4,6)                                           STAB 340
      C(N0+2,N0+3)=CJ(N,5,6)                                           STAB 350
      DO 31 J=1,N                                                      STAB 360
      J0=3*J                                                           STAB 370
      C(J0-2,J0+1)=CJ(J,4,1)                                           STAB 380
      C(J0-1,J0+1)=CJ(J,4,2)                                           STAB 390
      C(J0  ,J0+1)=CJ(J,4,3)                                           STAB 400
      C(J0-2,J0+2)=CJ(J,5,1)                                           STAB 410
      C(J0-1,J0+2)=CJ(J,5,2)                                           STAB 420
      C(J0  ,J0+2)=CJ(J,5,3)                                           STAB 430
      C(J0-2,J0+3)=CJ(J,6,1)                                           STAB 440
      C(J0-1,J0+3)=CJ(J,6,2)                                           STAB 450
      C(J0  ,J0+3)=CJ(J,6,3)                                           STAB 460
   31 CONTINUE                                                         STAB 470
      DO 32 J=2,N                                                      STAB 480
      J0=3*J                                                           STAB 490
      C(J0-2,J0-2)=CJ(J,1,1)+CJ(J-1,4,4)                               STAB 500
      C(J0-1,J0-1)=CJ(J,2,2)+CJ(J-1,5,5)                               STAB 510
      C(J0  ,J0  )=CJ(J,3,3)+CJ(J-1,6,6)                               STAB 520
      C(J0-2,J0-1)=CJ(J,1,2)+CJ(J-1,4,5)                               STAB 530
      C(J0-2,J0  )=CJ(J,1,3)+CJ(J-1,4,6)                               STAB 540
      C(J0-1,J0  )=CJ(J,2,3)+CJ(J-1,5,6)                               STAB 550
   32 CONTINUE                                                         STAB 560
      DO 42 J=1,N1                                                     STAB 570
      DO 41 K=1,J                                                      STAB 580
      C(J,K)=C(K,J)                                                    STAB 590
   41 CONTINUE                                                         STAB 600
```

```
110      42 CONTINUE                                                    STAB 610
111         DO 220 J=1,N1
112         DO 220 I=1,N1
113     220 A(I,J)=C(I,J)
114         DO 301 I=1,N1                                               STAB1110
115         DO 301 J=1,N1                                               STAB1120
116         CC(I,J)=0.0                                                 STAB1130
117         DO 301 K=1,N1                                               STAB1140
118     301 CC(I,J)=CC(I,J)+C(I,K)*V(K,J)                               STAB1150
119         DO 302 I=1,N1
120         DO 302 J=1,N1
121         C(I,J)=0.0
122         DO 302 K=1,N1
123     302 C(I,J)=C(I,J)+V(K,I)*CC(K,J)
124         DO 52 J=1,N1
125         RHO(J)=DSQRT(RHO(J))
126      52 CONTINUE
127         DO 55 I=1,N1
128         DO 54 J=1,N1
129         C(I,J)=C(I,J)/(RHO(I)*RHO(J))
130      54 CONTINUE
131      55 CONTINUE
132         DO 600 I=1,N1                                               STAB
133         DO 599 J=1,N1                                               STAB
134         D(I,J)=D(I,J)*RHO(J)
135     599 CONTINUE                                                    STAB
136     600 CONTINUE                                                    STAB
137         DO 1002 I=1,N1
138         DO 1002 J=1,I
139    1002 C(I,J)=C(J,I)
140    2000 CALL JACOBD(C,NJC,N1,EPS,V,ILL)
141         IF(ILL.NE.0) GO TO 100                                      STAB 760
142         DO 610 J=1,N1                                               STAB
143         EIG(J)=C(J,J)                                               STAB
144     610 CONTINUE                                                    STAB
145         WRITE(6,75)
146         WRITE(6,80) (EIG(J),J=1,N1)
147         DO 603 I=1,N1                                               STAB
148         DO 602 J=1,N1                                               STAB
149         C(I,J)=0.0
150         DO 601 K=1,N1                                               STAB
151         C(I,J)=C(I,J)+D(I,K)*V(K,J)
152     601 CONTINUE                                                    STAB
153     602 CONTINUE                                                    STAB
154     603 CONTINUE                                                    STAB
155         DO 60 J=1,N1                                                STAB 770
156         IF(EIG(J).GT.0.000001) GO TO 60
157         DO 62 I=1,N+1                                               STAB 810
158         IO=3*I                                                      STAB 820
159         IN1=IO-1                                                    STAB 830
160         IN2=IO-2                                                    STAB 840
161         PX1(I)=C(IN2,J)                                             STAB
162         PX2(I)=C(IN1,J)                                             STAB
163         PX3(I)=C(IO ,J)                                             STAB
164      62 CONTINUE                                                    STAB 880

165         CCC=EIG(J)                                                  STAB
166         WRITE(6,61) CCC
167         WRITE(6,81)
168         WRITE(6,80) (PX1(I),I=1,N+1)                                STAB 883
169         WRITE(6,82)
170         WRITE(6,80) (PX2(I),I=1,N+1)                                STAB 884
171         WRITE(6,83)
172         WRITE(6,80) (PX3(I),I=1,N+1)                                STAB 885
173         IF(CCC.GT.0.0) GO TO 60                                     STAB 800
174         PX1(N-KZ+1)=PX1(N+1)
175         PX2(N-KZ+1)=PX2(N+1)
176         PX3(N-KZ+1)=PX3(N+1)
177         NKZ=N-KZ+1
178         CALL PLOT2(XY7,-1,PX1,-1,NKZ)
179         WRITE(6,91)                                                 STAB 897
180         CALL PLOT2(PX2,-1,PX3,-1,NKZ)
181      60 CONTINUE                                                    STAB 910
182         GO TO 102                                                   STAB 920
183     100 WRITE(6,70) ILL                                             STAB 930
184     102 CONTINUE
185         RETURN
186         END
```

```
      SUBROUTINE CJRHO(CJ,RJ,H,N,KZ)
      COMMON/HEI/@A,ASP,A1,A2,A3,SS,SK,ST,DL
      COMMON/FX/SN,SM,RRMO                                              STAB  20
      COMMON/INT/GX(20),GA(20)
      DIMENSION F(6,6),G(6,6),CJ(50,6,6),RJ(50,6,6)
      DOUBLE PRECISION CJ,RJ,X,A,B,AX1,AX2,AX3,BB1,BB2,BB3,CC1,CC2,CC3,
     1                 DD1,DD2,DD3,DD4,FF1,FF2,FF3,FF4,F,G,GX,GA
      DATA (GX(I),I=11,20)/                                             GSS20 30
     1 0.07652652113349?,0.22778585114164?,0.37?706088715419,
     2 0.5108670019508?7,0.636053680726515,0.7463319?06460150,          GSS20 50
     3 0.839116971822218,0.912234428251325,0.963971927277913,           GSS20 60
     4 0.993128599185094/                                               GSS20 70
      DATA (GA(I),I=11,20)/                                             GSS20 80
     1 0.152753387130725,0.14917298047260?,0.142096109318382,           GSS20 90
     2 0.131688638449176,0.118194531961518,0.101930119817240,          GSS20100
     3 0.083276741576704,0.062672048334109,0.040601429800386,          GSS20110
     4 0.017614007139152/                                               GSS20120
      DO 1111 I=1,10                                                    GSS20130
      II=21-I                                                           GSS20140
      GX(I)=-GX(II)                                                     GSS20150
      GA(I)= GA(II)                                                     GSS20160
1111  CONTINUE
      H0=H
      DO 1 I=1,N                                                        MXCJ  90
      IF(I.EQ.N) GO TO 10
      IF(I.LT.N-KZ) GO TO 11
      H=H*0.5
      B=A
      A=A+H
      GO TO 20
   11 A=H*I
      B=A-H
      GO TO 20
   10 B=A
      A=1.0
      H=A-B
   20 CONTINUE
      DO 3 J=1,6                                                        MXCJ 120
      DO 2 K=1,6
      CJ(I,J,K)=0.0                                                     MXCJ 140
      RJ(I,J,K)=0.0                                                     MXCJ 145
    2 CONTINUE                                                          MXCJ 150
    3 CONTINUE
      CN=0.5*(A-B)                                                      MXCJ 170
      CP=0.5*(A+B)                                                      MXCJ 180
      DO 4 J=1,20
      X=CN*GX(J)+CP                                                     MXCJ 200
      CALL COEF(X,A,B,H,AX1,AX2,AX3,BB1,BB2,BB3,CC1,CC2,CC3,CC4,DD1,DD2,MXCJ 210
     1          DD3,DD4)                                                MXCJ 220
      CALL FG(X,F)                                                      MXCJ 230
      CJ(I,1,1)=CJ(I,1,1)+CN*GA(J)*(F(1,1)*AX1+F(4,4)*BB1+2.0*F(1,4)*DD1MXCJ 240
     1)                                                                 MXCJ 245
      CJ(I,2,2)=CJ(I,2,2)+CN*GA(J)*F(2,2)*AX1                           MXCJ 250
      CJ(I,3,3)=CJ(I,3,3)+CN*GA(J)*F(3,3)*AX1                           MXCJ 260
      CJ(I,4,4)=CJ(I,4,4)+CN*GA(J)*(F(1,1)*AX3+F(4,4)*BB3+2.0*F(1,4)*DD4MXCJ 270

     1)                                                                 MXCJ 275
      CJ(I,5,5)=CJ(I,5,5)+CN*GA(J)*F(2,2)*AX3                           MXCJ 280
      CJ(I,6,6)=CJ(I,6,6)+CN*GA(J)*F(3,3)*AX3                           MXCJ 290
      CJ(I,2,1)=CJ(I,2,1)+CN*GA(J)*(F(1,2)*CC1+F(2,4)*DD1)              MXCJ 300
      CJ(I,3,1)=CJ(I,3,1)+CN*GA(J)*(F(1,3)*CC1+F(3,4)*DD1)              MXCJ 310
      CJ(I,4,1)=CJ(I,4,1)+0.5*CN*GA(J)*(F(1,1)*AX2+F(4,4)*BB2+2.0*F(1,4)MXCJ 320
     1          *(DD2+DD3))                                             MXCJ 325
      CJ(I,5,1)=CJ(I,5,1)+CN*GA(J)*(F(1,2)*CC2+F(2,4)*DD3)              MXCJ 330
      CJ(I,6,1)=CJ(I,6,1)+CN*GA(J)*(F(1,3)*CC2+F(3,4)*DD3)              MXCJ 340
      CJ(I,3,2)=CJ(I,3,2)+CN*GA(J)*F(2,3)*CC1                           MXCJ 350
      CJ(I,4,2)=CJ(I,4,2)+CN*GA(J)*(F(1,2)*CC3+F(2,4)*DD2)              MXCJ 360
      CJ(I,5,2)=CJ(I,5,2)+0.5*CN*GA(J)*F(2,2)*AX2                       MXCJ 370
      CJ(I,6,2)=CJ(I,6,2)+CN*GA(J)*F(2,3)*CC2                           MXCJ 380
      CJ(I,4,3)=CJ(I,4,3)+CN*GA(J)*(F(1,3)*CC3+F(3,4)*DD2)              MXCJ 390
      CJ(I,5,3)=CJ(I,5,3)+CN*GA(J)*F(2,3)*CC3                           MXCJ 400
      CJ(I,6,3)=CJ(I,6,3)+0.5*CN*GA(J)*F(3,3)*AX2                       MXCJ 410
      CJ(I,5,4)=CJ(I,5,4)+CN*GA(J)*(F(1,2)*CC4+F(2,4)*DD4)              MXCJ 420
      CJ(I,6,4)=CJ(I,6,4)+CN*GA(J)*(F(1,3)*CC4+F(3,4)*DD4)              MXCJ 430
      CJ(I,6,5)=CJ(I,6,5)+CN*GA(J)*F(2,3)*CC4                           MXCJ 440
      RJ(I,1,1)=RJ(I,1,1)+CN*GA(J)*F(6,6)*AX1                           MXCJ 241
      RJ(I,4,1)=RJ(I,4,1)+0.5*CN*GA(J)*F(6,6)*AX2                       MXCJ 243
      RJ(I,4,4)=RJ(I,4,4)+CN*GA(J)*F(6,6)*AX3                           MXCJ 242
      RJ(I,2,2)=RJ(I,1,1)
      RJ(I,3,3)=RJ(I,1,1)
      RJ(I,5,5)=RJ(I,4,4)
      RJ(I,6,6)=RJ(I,4,4)
      RJ(I,5,2)=RJ(I,4,1)
      RJ(I,6,3)=RJ(I,4,1)
    4 CONTINUE                                                          MXCJ 450
      DO 6 J=1,6                                                        MXCJ 460
      DO 5 K=1,J                                                        MXCJ 470
      CJ(I,K,J)=CJ(I,J,K)                                               MXCJ 480
      RJ(I,K,J)=RJ(I,J,K)                                               MXCJ 495
    5 CONTINUE                                                          MXCJ 490
    6 CONTINUE                                                          MXCJ 500
    1 CONTINUE                                                          MXCJ 510
      CALL SSVV(SV)
      CJ(N,4,4)=CJ(N,4,4)+SV
      H=H0
      RETURN                                                            MXCJ 520
      END                                                               MXCJ 530
```

```
      SUBROUTINE COEF(X,A,B,H,AA1,AA2,AA3,BB1,BB2,BB3,CC1,CC2,CC3,CC4,DDCOEF  10
     1               1,DD2,DD3,DD4)                                    COEF  20
      DOUBLE PRECISION CJ,RJ,X,A,B,AA1,AA2,AA3,BB1,BB2,BB3,CC1,CC2,CC3,
     1                 DD1,DD2,DD3,DD4,FF1,FF2,FF3,FF4
      XX=A-X                                                           COEF  30
      YY=B-X                                                           COEF  40
      HI=1.0/H                                                         COEF  50
      HI2=HI**2                                                        COEF  60
      AA1=XX**2*HI2                                                    COEF  70
      AA2=-2.0*XX*YY*HI2                                               COEF  80
      AA3=YY**2*HI2                                                    COEF  90
      BB1=HI2                                                          COEF 100
      BB2=-2.0*HI2                                                     COEF 110
      BB3=BB1                                                          COEF 120
      CC1=AA1                                                          COEF 130
      CC2=0.5*AA2                                                      COEF 140
      CC3=CC2                                                          COEF 150
      CC4=AA3                                                          COEF 160
      DD1=-XX*HI2                                                      COEF 170
      DD2=-DD1                                                         COEF 180
      DD3= YY*HI2                                                      COEF 190
      DD4=-DD3                                                         COEF 200
      RETURN                                                           COEF 240
      END                                                              COEF 250
```

```
      SUBROUTINE FG(R,F)                                               FG    10
      COMMON/HEI/@4,ASP,A1,A2,A3,SS,SK,ST,DL
      COMMON/FX/SN,SM,RRHO                                             STAB  20
      COMMON/GGG/GAM
      DIMENSION F(6,6)                                                 FG    35
      DOUBLE PRECISION AK,RK,RK2,SM2,RKM,BTK,BTM,BPK,BPM,BKM,
     1                 R,BT,BP,CJT,CJP,P,PDR,F
      AK=SN/ASP                                                        FG    40
      DO 2 I=1,6
      DO 1 J=1,6                                                       FG    51
      F(I,J)=0.0                                                       FG    52
    1 CONTINUE                                                         FG    53
    2 CONTINUE                                                         FG    54
      CALL HEIKO(R,BT,BP,CJT,CJP,P,PDR)                                FG    60
      RK=AK*R                                                          FG    70
      RK2=RK*RK                                                        FG    80
      SM2=SM*SM                                                        FG    90
      RKM=RK2+SM2                                                      FG   100
      BTK=RK*BT                                                        FG   110
      BTM=SM*BT                                                        FG   120
      BPK=RK*BP                                                        FG   130
      BPM=SM*BP                                                        FG   140
      F(1,1)=GAM    *P/R+(BP**2+BT**2)/R          +((BTK+BPM)**2-2.*BP*RFG   150
     1       *CJT)/R                                                   FG   160
      F(2,2)=GAM    *SM2*P/R+RKM*BT**2/R                               FG  1170
      F(3,3)=GAM    *P*RK2/R+RKM*BP**2/R                               FG   180
      F(4,4)=GAM    *R*P*R*(RK*BT+SM*BP)**2/RKM*R*(RK*BP-SM*BT)**2/RKM FG   190
      F(1,2)=GAM    *SM*P/R+(RK*BP+SM*BT)*BT/R                         FG   200
      F(2,3)=GAM    *AK*SM*P-RKM*BP*BT/R
      F(1,3)=GAM    *AK*P-(RK*BP+SM*BT)*BP/R                           FG   220
      F(1,4)=GAM    *P   +(RK2*BT**2-SM2*BP**2)/RKM-(RK2*BP**2-SM2*BT**2)FG   230
     1/RKM                                                             FG   240
      F(2,4)=GAM    *SM*P-(RK*BP-SM*BT)*BT                             FG   250
      F(3,4)=GAM    *RK*P+(RK*BP-SM*BT)*BP                             FG   260
      RH=1.0
      IF(R.GT.1.0) RH=RRHO
      F(6,6)=R*RH
      RETURN                                                           FG   270
      END                                                              FG   280
```

```
      SUBROUTINE SSVV(SV)
      COMMON/HEI/@A,ASP,A1,A2,A3,SS,SK,ST,DL
      COMMON/FX/SN,SM,RRHO
      COMMON/INT/GX(20),GA(20)
      COMMON/BB/B
      DOUBLE PRECISION R1,R2,R3,R4,BT1,BT2,BT3,BT4,BP1,BP2,BP3,BP4,
     1                 BT,BP,AJT,AJP,P,PDR,R,PDR1,X,GX,GA
      SV=0.0
      R=1.0
      SK=SN/ASP
      CALL        HEIKO(R,BT,BP,AJT,AJP,P,PDR1)
      C=RR*(SM+SN*@A)/SK
      C=C*C
      R1=0.9998
      R2=0.9999
      R3=1.0001
      R4=1.0002
      CALL        HEIKO(R1,BT1,BP1,AJT,AJP,P,PDR)
      CALL        HEIKO(R2,BT2,BP2,AJT,AJP,P,PDR)
      CALL        HEIKO(R3,BT3,BP3,AJT,AJP,P,PDR)
      CALL        HEIKO(R4,BT4,BP4,AJT,AJP,P,PDR)
      WA=-PDR1-0.5*(BP2**2-BP1**2+BT2**2-BT1**2+BP3**2-BP4**2
     1  +BT3**2-BT4**2)*10000.
      AS=SK
      BS=SK*B
      M=SM
      CALL BESI(AS,M+1,BIPA,IER)
      CALL BESI(AS,M-1,BIMA,IER)
      CALL BESI(BS,M+1,BIPB,IER)
      CALL BESI(BS,M-1,BIMB,IER)
      CALL BESK(AS,M+1,BKPA,IER)
      CALL BESK(AS,M-1,BKMA,IER)
      CALL BESK(BS,M+1,BKPB,IER)
      CALL BESK(BS,M-1,BKMB,IER)
      BKA=-0.5*(BKPA+BKMA)
      BKB=-0.5*(BKPB+BKMB)
      BIA=0.5*(BIPA+BIMA)
      BIB=0.5*(BIPB+BIMB)
      C1=BKA*BIB-BKB*BIA
      C1=C/C1/C1
      CI=BIB
      CK=-BKB
      A=1.0
      CN=0.5*(B-A)
      CP=0.5*(A+B)
      DO 4 J=1,20
      X=CN*GX(J)+CP
      AS=X*SK
      CALL BESI(AS,M+1,BIPA,IER)
      CALL BESI(AS,M-1,BIMA,IER)
      CALL BESI(AS,M,BI0,IER)
      CALL BESK(AS,M+1,BKPA,IER)
      CALL BESK(AS,M-1,BKMA,IER)
      CALL BESK(AS,M,BK0,IER)
      BKA=-0.5*(BKPA+BKMA)
      BIA=0.5*(BIPA+BIMA)
      CALL        HEIKO(X,BT,BP,AJT,AJP,P,PDR)
      SV1=SK**2*((CI*BKA+CK*BIA)**2+(SM*SM/X/X+SK*SK)*(CI*BK0+CK*BI0)**2
      SV1=SV1*X*C1
    4 SV=SV+CN*GA(J)*SV1
      WRITE(6,6) WA,SV
    6 FORMAT(1H ,F20.3,E20.3)
      SV=SV*WA
      RETURN
      END
```

```
      SUBROUTINE RHOX(B)
      COMMON /HEI/@A,ASP,A1,A2,A3,SS,SK,ST,DL
      COMMON/FX/SN,SM,RRHO                                              RHOX  30
      COMMON/XY/XYZ(50)
      DIMENSION PJ1(50),PJ2(50),BP1(50),PR(50),@A1(50),BT1(50),RR(50)
      DOUBLE PRECISION R,BT,BP,CJT,CJP,P,PDR
   14 FORMAT(1H ,' RADIUS          @          TOROIDAL FIELD      POLOIDAL
     1 FIELD          POLOIDAL FIELD      POL. CURRENT        TOR. CUR
     2RENT'/)
   15 FORMAT(1H ,2F11.2,5E20.3)
   20 FORMAT(1H1,'      TOROIDAL CURRENT',60X,' POLOIDAL CURRENT'/)       RHOX 252
   21 FORMAT(1H1,'                        ',60X,' PRESSURE'/)             RHOX 262
   22 FORMAT(1H1,'    SAFTY FAC.  '/)
      AK=SN/ASP                                                         RHOX  60
      J=0
      WRITE(6,14)
    1 J=J+1
      R=J=0.4999
      R=R+0.05
      CALL HEIKO(R,BT,BP,CJT,CJP,P,PDR)                                 RHOX 110
      RR(J)=R
      PJ1(J)=CJT                                                        RHOX 220
      PJ2(J)=CJP                                                        RHOX 230
      PR(J)=P                                                           RHOX 240
      BT1(J)=BT
      BP1(J)=BP                                                         RHOX 241
      @A1(J)=R*BT/BP/ASP                                                RHOX 243
      WRITE(6,15) RR(J),@A1(J),PR(J),BT1(J),BP1(J),PJ2(J),PJ1(J)
      IF(R.GE.2.0) GO TO 10
      IF(R.GE.B) GO TO 10
      IF(J.GE.50) GO TO 10
      GO TO 1                                                           RHOX 244
   10 @A1(J)=1.0
      WRITE(6,20)                                                       RHOX 251
      CALL PLOT2(PJ1,-1,PJ2,-1,J)
      WRITE(6,21)                                                       RHOX 261
      CALL PLOT2(XY7,-1,PR ,-1,J)
      WRITE(6,22)
      CALL PLOT2(@A1,-1,XYZ,-1,J)
      RETURN                                                            RHOX 270
      END                                                               RHOX 280


      SUBROUTINE HEIKO(R,BT,BP,AJT,AJP,P,PDR)                           HEIKO 10
      COMMON/HEI/@A,ASP,A1,A2,A3,SS,SK,ST,DL
      COMMON/FX/SN,SM,RRHO                                              STAB  20
      DOUBLE PRECISION BT,BP,AJT,AJP,P,PDR,R
      AA1=A1*(SS+2.0)/SS/ASP/@A**2.0                                    HEIKO 35
      SK2=SK**2                                                         HEIKO 40
      AA3=A3*(ST+2.0)*(ST+3.0)/ASP/@A                                   HEIKO 55
      IF(R.GT.1.0) GO TO 10                                             HEIKO 60
      BT=1.0-DL*(1.0-2.0*R**2+R**4)
      BP=AA1*(0.5-R**SS/(SS+2.0))*R                                     HEIKO 80
     1+AA3*R**(ST+1)*(1.0/(ST+2.0)-R/(ST+3.0))
      AJT=AA1*(1.0-R**SS)+AA3*R**ST*(1.-R)                              HEIKO 90
      AJP=-4.0*DL*R*(1.0-R**2)
      PDR=AJP*BT-AJT*BP                                                 HEIKO110
       S1=SS+1.                                                         HEIKO115
      S2=SS+2.                                                          HEIKO120
      S3=SS+3.                                                          HEIKO125
      S4=SS+4.                                                          HEIKO130
      T1=ST+1.                                                          HEIKO135
      T2=ST+2.                                                          HEIKO140
      T3=ST+3.                                                          HEIKO145
      T4=ST+4.                                                          HEIKO150
      T5=ST+5.                                                          HEIKO155
      RT=R**ST                                                          HEIKO160
      RS=R**SS                                                          HEIKO165
      P1=0.25-0.5*RS/S2*(S4/S2-RS/S1)                                   HEIKO170
      P2=0.5/T1-(T1+T4)*R/T3/(T1+T2)+0.5*R*R/T3                         HEIKO175
      P3=0.5*T4/T2/T2-0.5*R*T5/T3/T3-RS*(T2+S2)/T2/S2/(S1+T1)           HEIKO180
     1+RS*R*(T2+S3)/T3/S2/(S1+T2)                                       HEIKO185
      P=-AA1*AA1*R*R*P1-AA3*AA3*RT*RT*R*R/T2*P2-AA1*AA3*RT*R*R*P3       HEIKO190
      P=P-2.0*DL*(1.0-DL)*R**2+DL*(1.0-3.0*DL)*R**4+2.0*DL**2*R**6-0.5*D
     1L**2*R**8
      P=P+AA3**2/T2*(0.5/T1-(T2+T3)/T3/(T1+T2)+0.5/T3)                  HEIKO205
      P=P+AA1**2*(0.25-S4*0.5/S2/S2+0.5/S2/S1)                          HEIKO200
      P=P+AA1*AA3*(0.5*T4/T2/T2-T5/T3/T3*0.5-(T2+S2)/T2/S2/(S1+T1)+     HEIKO210
     1(T2+S3)/T3/S2/(S1+T2))                                            HEIKO215
      P=P+DL*(1.0-0.5*DL)
      RETURN                                                            HEIKO220
   10 BT=1.0                                                            HEIKO230
      BP=1./ASP/@A/R                                                    HEIKO240
      PDR=0.0                                                           HEIKO250
      P=0.0                                                             HEIKO260
      AJT=0.0                                                           HEIKO270
      AJP=0.0                                                           HEIKO280
      RETURN                                                            HEIKO290
      END                                                               HEIKO300
```

PLASMA RADIUS = 1.0 , WALL---B= 1.43000

N = 1 / 3 K= 10

RADIUS=H*(I-1) H=1.0/N (I.LE.N-K) H=H*0.5 (I.GT.N-K)

GAMMA= 1.6667E 00

SN,SM,@A,ASP= 1.00000 -2.00000 1.90000 5.00000
A1,A2,A3,SS,S_K,ST= 1.00000 0.0 0.0 20.00000 1.00000 1.00000
DL= -0.00010
RRHO= 0.00100

JZ =A1*(SS+2)/SS/ASP/@A*2*(1-R**SS)+A3*(ST+2)*(ST+3)/ASP/@A*R**ST*(1-R)

RADIUS	@	TOROIDAL FIELD	POLOIDAL FIELD	POLOIDAL FIELD	POL. CURRENT	TOR. CURRENT
0.50E-05	0.17E 01	0.120E-01	0.100E 01	0.579E-06	0.200E-08	0.232E 00
0.50E-01	0.17E 01	0.120E-01	0.100E 01	0.579E-02	0.200E-04	0.232E 00
0.10E 00	0.17E 01	0.119E-01	0.100E 01	0.116E-01	0.396E-04	0.232E 00
0.15E 00	0.17E 01	0.117E-01	0.100E 01	0.174E-01	0.587E-04	0.232E 00
0.20E 00	0.17E 01	0.115E-01	0.100E 01	0.232E-01	0.768E-04	0.232E 00
0.25E 00	0.17E 01	0.112E-01	0.100E 01	0.289E-01	0.938E-04	0.232E 00
0.30E 00	0.17E 01	0.108E-01	0.100E 01	0.347E-01	0.109E-03	0.232E 00
0.35E 00	0.17E 01	0.104E-01	0.100E 01	0.405E-01	0.123E-03	0.232E 00
0.40E 00	0.17E 01	0.992E-02	0.100E 01	0.463E-01	0.134E-03	0.232E 00
0.45E 00	0.17E 01	0.936E-02	0.100E 01	0.521E-01	0.144E-03	0.232E 00
0.50E 00	0.17E 01	0.873E-02	0.100E 01	0.579E-01	0.150E-03	0.232E 00
0.55E 00	0.17E 01	0.803E-02	0.100E 01	0.637E-01	0.153E-03	0.232E 00
0.60E 00	0.17E 01	0.727E-02	0.100E 01	0.695E-01	0.154E-03	0.232E 00
0.65E 00	0.17E 01	0.644E-02	0.100E 01	0.753E-01	0.150E-03	0.232E 00
0.70E 00	0.17E 01	0.554E-02	0.100E 01	0.810E-01	0.143E-03	0.231E 00
0.75E 00	0.17E 01	0.458E-02	0.100E 01	0.868E-01	0.131E-03	0.231E 00
0.80E 00	0.17E 01	0.355E-02	0.100E 01	0.925E-01	0.115E-03	0.229E 00
0.85E 00	0.17E 01	0.248E-02	0.100E 01	0.981E-01	0.943E-04	0.223E 00
0.90E 00	0.17E 01	0.140E-02	0.100E 01	0.103E 00	0.684E-04	0.203E 00
0.95E 00	0.18E 01	0.458E-03	0.100E 01	0.106E 00	0.370E-04	0.149E 00
0.10E 01	0.19E 01	0.0	0.100E 01	0.105E 00	0.0	0.0
0.11E 01	0.21E 01	0.0	0.100E 01	0.100E 00	0.0	0.0
0.11E 01	0.23E 01	0.0	0.100E 01	0.957E-01	0.0	0.0
0.12E 01	0.25E 01	0.0	0.100E 01	0.915E-01	0.0	0.0
0.12E 01	0.27E 01	0.0	0.100E 01	0.877E-01	0.0	0.0
0.13E 01	0.30E 01	0.0	0.100E 01	0.842E-01	0.0	0.0
0.13E 01	0.32E 01	0.0	0.100E 01	0.810E-01	0.0	0.0
0.14E 01	0.35E 01	0.0	0.100E 01	0.780E-01	0.0	0.0
0.14E 01	0.37E 01	0.0	0.100E 01	0.752E-01	0.0	0.0
0.15E 01	0.40E 01	0.0	0.100E 01	0.726E-01	0.0	0.0

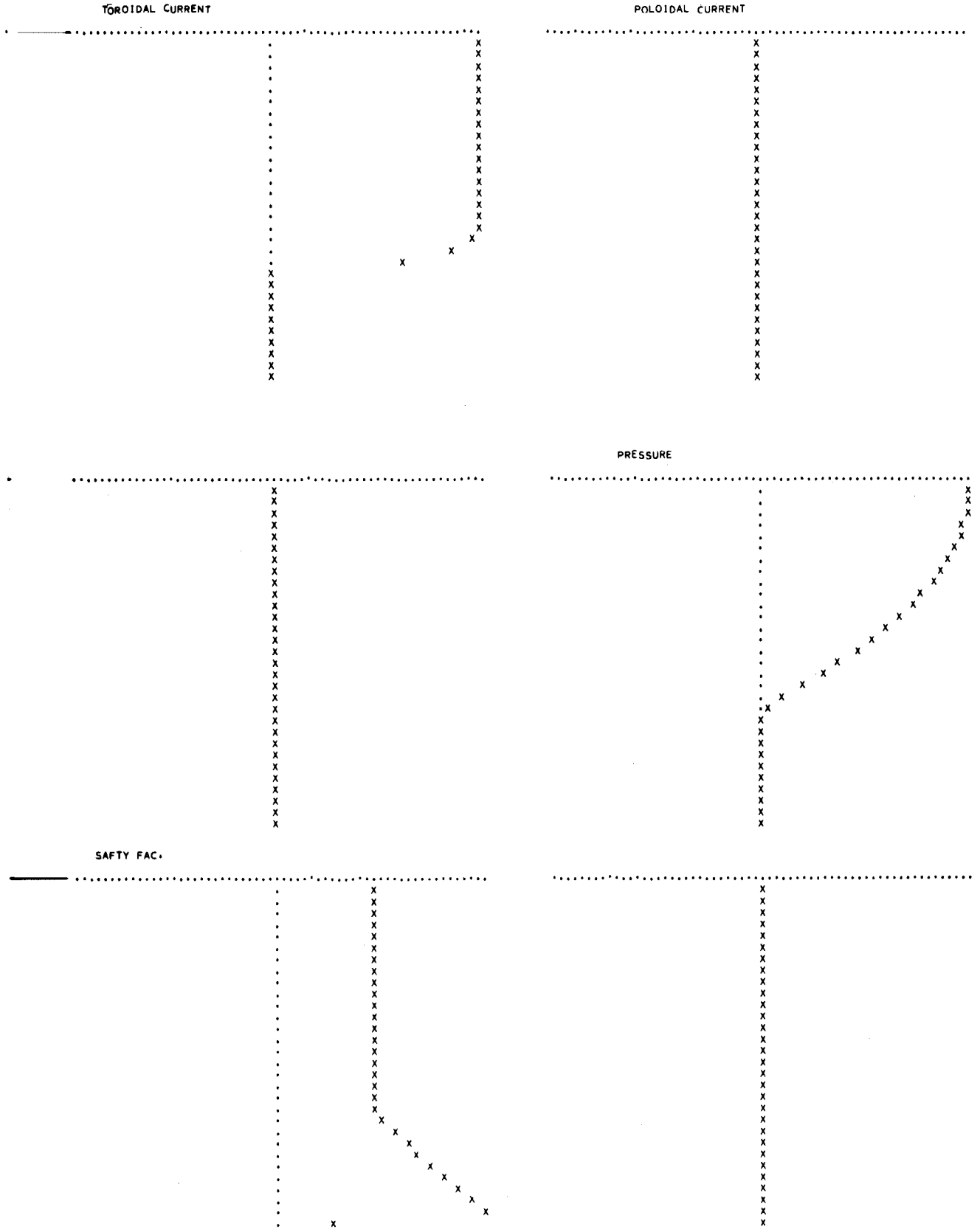
TOROIDAL CURRENT
POLOIDAL CURRENT
PRESSURE
SAFTY FAC.

```
      -0.646E-04          0.0
 ILL=       0

     EIGEN VALUE

         7.5642E 02  1.8760E 04  2.4044E-02  4.0405E 01  8.2542E-04  6.5081E-04  5.6414E 02 -2.0354E-03  2.0762E-04  4.1527E 02
         2.7208E 00  4.9165E-05  2.6473E 02  3.5753E 00  1.0150E-04  2.7054E 01  1.1293E 01  1.0126E-05  1.5155E 02  8.0273E-01
         2.1982E-05  7.5028E 01  5.5164E 00  3.1343E-06  1.7594E 03  1.1277E-01  3.5958E-07  7.1770E 03  3.5866E-01  3.0571E-08
         2.8936E 04  1.6979E 00  2.8290E-07

IGEN VALUE  = -2.0354E-03

   EIGEN FUNCTION   R
         4.2880E-04  5.2860E-03  1.8032E-02  3.8913E-02  6.7929E-02  1.0508E-01  1.0647E-01  6.4146E-02  3.5010E-02  2.4502E-02
         1.2547E-02

   EIGEN FUNCTION   THETA
         3.8382E-04  5.0121E-03  1.7452E-02  3.7924E-02  6.6308E-02  1.0244E-01  1.0356E-01  6.2281E-02  3.3980E-02  2.3792E-02
         1.2187E-02

   EIGEN FUNCTION   Z
        -1.7815E-05 -1.2752E-04 -5.8876E-04 -1.8481E-03 -4.2896E-03 -8.3332E-03 -9.8296E-03 -6.4641E-03 -3.6147E-03 -2.5311E-03
        -1.2896E-03
```

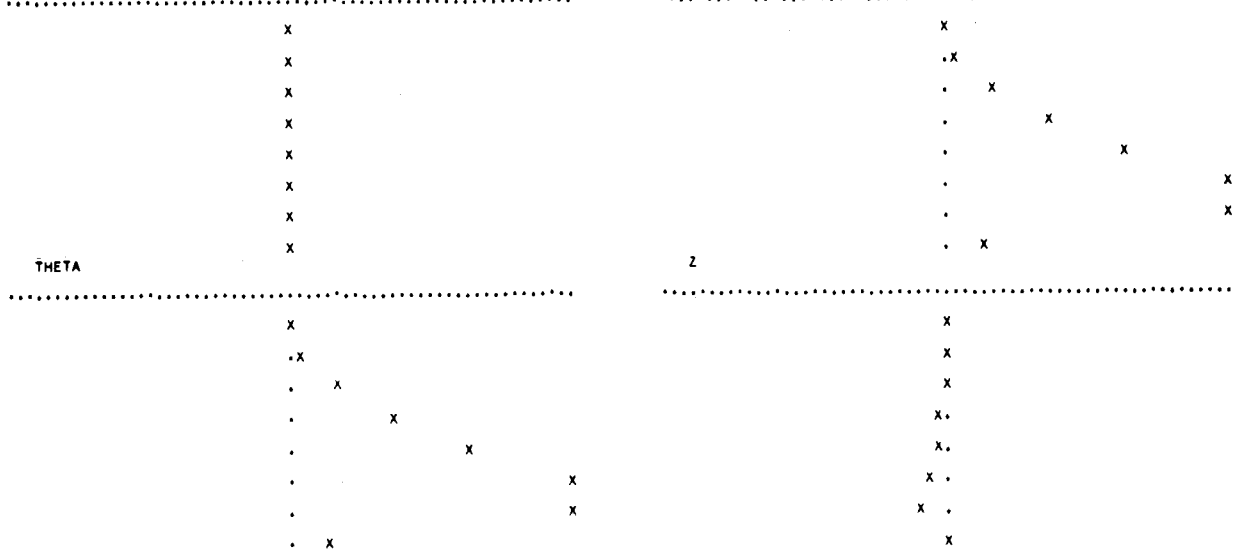


```
IGEN VALUE  = 3.1343E-06

   EIGEN FUNCTION   R
         7.2001E-06  3.4323E-05  4.4889E-05  3.1720E-05 -4.6791E-07 -4.2666E-05 -5.1667E-05 -1.5572E-05 -9.4520E-06 -8.1851E-06
        -4.4235E-06

   EIGEN FUNCTION   THETA
         4.2743E-06  2.7307E-05  6.9771E-05  2.0792E-04  7.3391E-04  2.6410E-03  9.8985E-03  1.7916E-02 -2.0316E-04 -2.2960E-05
        -3.3809E-05

   EIGEN FUNCTION   Z
         1.4970E-04  9.1962E-04  2.1022E-03  4.6298E-03  1.1819E-02  3.2207E-02  9.8940E-02  1.7126E-01 -1.1339E-03  5.7281E-05
        -1.9822E-04

IGEN VALUE  = 3.5958E-07

   EIGEN FUNCTION   R
         4.5787E-07  2.2016E-06  2.9051E-06  1.9814E-06 -5.5213E-07 -4.6512E-06 -6.7916E-06 -3.9447E-06 -3.3756E-07  3.0984E-07
        -1.4705E-07

   EIGEN FUNCTION   THETA
         1.9871E-07  6.8028E-07 -8.5778E-09 -1.9077E-06 -3.7066E-06 -3.1708E-07  6.5184E-05  4.2248E-03  1.0727E-02 -2.1291E-03
         2.9650E-03

   EIGEN FUNCTION   Z
         4.7488E-07  2.9446E-06  6.8864E-06  1.5956E-05  4.4574E-05  1.3907E-04  7.6463E-04  3.9636E-02  1.0036E-01 -1.9842E-02
         2.8295E-02

IGEN VALUE  = 3.0571E-08

   EIGEN FUNCTION   R
        -4.4158E-08 -2.0053E-07 -2.2374E-07 -5.2972E-08  3.1311E-07  8.7744E-07  1.1258E-06  7.4564E-07  3.1584E-07  2.0938E-08
        -2.4294E-08

   EIGEN FUNCTION   THETA
        -1.7874E-08 -4.1270E-08  1.0090E-07  4.5768E-07  1.0934E-06  2.2491E-06  5.8070E-06 -1.4026E-04  1.6878E-03  1.0372E-02
         5.7806E-03

   EIGEN FUNCTION   Z
         2.1464E-08  1.3108E-07  3.0903E-07  7.4844E-07  2.1524E-06  6.6884E-06  3.8675E-05 -1.3218E-03  1.5847E-02  9.7537E-02
         5.4648E-02

IGEN VALUE  = 2.8290E-07

   EIGEN FUNCTION   R
        -3.6146E-07 -1.4442E-06 -8.9614E-07  1.8252E-06  6.7182E-06  1.3777E-05  1.5906E-05  9.8234E-06  4.4240E-06  2.4976E-06
         7.3188E-07

   EIGEN FUNCTION   THETA
        -1.3601E-07 -9.6428E-08  1.7808E-06  5.7649E-06  1.1600E-05  1.8165E-05  4.3553E-06 -2.3667E-03 -8.6859E-03 -4.3738E-03
         4.7773E-03

   EIGEN FUNCTION   Z
        -7.1219E-08 -4.4664E-07 -1.0768E-06 -2.3895E-06 -7.4230E-06 -2.6602E-05 -1.6867E-04 -2.2277E-02 -8.1379E-02 -4.0667E-02
         4.553BE-02
```

D-3 Input data format for Code III

Card	Input data FORMAT						
1	6	N_1	N_0				
	F10.5	I10	I10				
2	n	m	q_a	$L/2\pi a$			
	F10.5	F10.5	F10.5	F10.5			
3	j_1	(0.0)	j_2	S	(0.0)	t	(0.0)
	F10.5	F10.5	F10.5	F10.5	F10.5	F10.5	F10.5

References

1. R. J. Tayler, Proc. Phys. Soc. (London) B70, 1049 (1957).
2. I. B. Bernstein, E. A. Frieman, M. D. Kruskal, and R. M. Kulsrud, Proc. Roy. Soc. (London) A224, 17 (1958).
3. B. R. Suydam, in Proceedings of the Second International Conference on the Peaceful Uses of Atomic Energy, (United Nations, Geneva, 1958) vol. 31, 157.
4. W. A. Newcomb, Ann. Phys. (N.Y.) 10, 232 (1960).
5. V. D. Shafranov, Zh. Tekh. Fiz. 40, 241 (1970), Sov. Phys. Tech. Phys. 15, 175 (1970).
6. D. M. Copley and K. J. Whiteman, Plasma Phys. 4, 103 (1962).
7. H. A. B. Bodin, E. P. Butt, J. E. Crow, F. E. Irons, J. Junker, A. A. Newton, and D. C. Robinson, in Plasma Physics and Controlled Nuclear Fusion Research (International Atomic Energy Agency, Vienna, 1971) Vol. 1, 225.
8. N. K. Winsor, E. C. Bowers, M. A. Hellberg, J. M. Dawson, ibid. Vol. 2, 393.
9. J. P. Boris, a paper presented in the Sherwood Theoretical Meeting (Princeton, N. J., April 1970).
10. N. J. Zabusky and G. S. Deem, J. Fluid Mech. 47, 353 (1971).
11. O. C. Zienkiewicz, in The Finite Element Method (McGraw Hill Publishing Company, 1967).
12. B. Langefors, J. Aero. Sci. 19, 451 (1952).
13. J. H. Argyris, Aircraft Engineering, 27, 125 (1955).
14. M. Ohta, Y. Shimomura and T. Takeda, Nucl. Fusion, 12, 271 (1972).
15. T. Takeda, Y. Shimomura, M. Ohta and M. Yoshikawa, Phys. Fluids, (to be published).
16. In Eq. (5) of Ref. 5 the absolute value brackets should be inserted for the first term in the backet as shown in Eq.(31) of this article. When the correction is made a single-peaked curve for the growth rate in Fig. 1a of Ref. 5 becomes a double-peaked one as shown in Figs. 1 and 2 of this article.

Table 1 Matrix $(\tilde{C}_i)_{\alpha\beta}$

α \ β	1	2	3	4	5	6
1	$f_{11}U_1+f_{44}V_1+2f_{14}W_1$	$f_{12}U_1+f_{24}W_1$	$f_{13}U_1+f_{34}W_1$	$\frac{1}{2}\{f_{11}(U_2+U_3)$ $+f_{44}(V_2+V_3)+2f_{14}(W_2+W_3)\}$	$f_{12}U_3+f_{24}W_2$	$f_{13}U_3+f_{34}W_2$
2	$f_{12}U_1+f_{24}W_1$	$f_{22}U_1$	$f_{23}U_1$	$f_{12}U_2+f_{24}W_3$	$\frac{1}{2}f_{22}(U_2+U_3)$	$f_{23}U_3$
3	$f_{13}U_1+f_{34}W_1$	$f_{23}U_1$	$f_{33}U_1$	$f_{13}U_2+f_{34}W_3$	$f_{23}U_2$	$\frac{1}{2}f_{33}(U_2+U_3)$
4	$\frac{1}{2}\{f_{11}(U_2+U_3)$ $+f_{44}(V_2+V_3)+2f_{14}(W_2+W_3)\}$	$f_{12}U_2+f_{24}W_3$	$f_{13}U_2+f_{34}W_3$	$f_{11}U_4+f_{44}V_4+2f_{14}W_4$	$f_{12}U_4+f_{24}W_4$	$f_{13}U_4+f_{34}W_4$
5	$f_{12}U_3+f_{24}W_2$	$\frac{1}{2}f_{22}(U_2+U_3)$	$f_{23}U_2$	$f_{12}U_4+f_{24}W_4$	$f_{22}U_4$	$f_{23}U_4$
6	$f_{13}U_3+f_{34}W_2$	$f_{23}U_3$	$\frac{1}{2}f_{33}(U_2+U_3)$	$f_{13}U_4+f_{34}W_4$	$f_{23}U_4$	$f_{44}U_4$

$$f_{11} = r\frac{P}{r} + \frac{1}{r}(B_\theta^2+B_Z^2) + \frac{1}{r}\left[(krB_Z+mB_\theta)^2 - 2B_\theta\frac{d}{dr}(rB_\theta)\right],$$

$$f_{22} = m^2 r\frac{P}{r} + \frac{1}{r}(k^2r^2+m^2)B_Z^2, \qquad f_{33} = k^2 rrP + \frac{1}{r}(k^2r^2+m^2)B_\theta^2, \qquad f_{44} = rrP + r(B_\theta^2+B_Z^2),$$

$$f_{12} = mr\frac{P}{r} + \frac{1}{r}(krB_\theta+mB_Z)B_Z, \qquad f_{23} = kmrP - \frac{1}{r}(k^2r^2+m^2)B_\theta B_Z, \qquad f_{13} = krP - \frac{1}{r}(krB_\theta+mB_Z)B_\theta,$$

$$f_{14} = rP + (B_\theta^2+B_Z^2), \qquad f_{24} = mrP - (krB_\theta-mB_Z)B_Z, \qquad f_{34} = krrP + (krB_\theta-mB_Z)B_\theta,$$

$$U_1 = \frac{x^2}{h}, \quad U_2 = -\frac{xy}{h^2}, \quad U_3 = -\frac{xy}{h^2}, \quad U_4 = \frac{y^2}{h^2}, \quad V_1 = \frac{1}{h^2}, \quad V_2 = -\frac{1}{h^2}, \quad V_3 = -\frac{1}{h^2}, \quad V_4 = \frac{1}{h^2},$$

$$W_1 = -\frac{x}{h^2}, \quad W_2 = \frac{y}{h^2}, \quad W_3 = \frac{x}{h^2}, \quad W_4 = -\frac{y}{h^2}, \quad x = r_{i+1}-r, \quad y = r_i-r, \quad h = r_{i+1}-r_i.$$

Table 2 Matrix $(\tilde{R}_i)_{\alpha\beta}$

α \ β	1	2	3	4	5	6
1	gU_1	0	0	$\frac{1}{2}g(U_2+U_3)$	0	0
2	0	gU_1	0	0	$\frac{1}{2}g(U_2+U_3)$	0
3	0	0	gU_1	0	0	$\frac{1}{2}g(U_2+U_3)$
4	$\frac{1}{2}g(U_2+U_3)$	0	0	gU_4	0	0
5	0	$\frac{1}{2}g(U_2+U_3)$	0	0	gU_4	0
6	0	0	$\frac{1}{2}g(U_2+U_3)$	0	0	gU_4

$g = 2\rho_p r$

U_μ, $(\mu = 1, 2, 3, 4)$ are given in Table 1.

Table 3 Matrix $(\widetilde{H}_i)_{\alpha\beta}$

α \ β	1	2	3	4	5	6
1	$A_{11}U_1$	$A_{12}U_1+A_{15}W_1$	$A_{16}W_1$	$\frac{1}{2}A_{11}(U_2+U_3)$	$A_{12}U_3+A_{15}W_3$	$A_{16}W_3$
2	$A_{12}U_1+A_{15}W_1$	$A_{22}U_1+A_{55}V_1+2A_{25}W_1$	$A_{23}U_1$	$A_{12}U_2+A_{15}W_2$	$\frac{1}{2}\{A_{22}(U_2+U_3)$ $+A_{55}(V_2+V_3)$ $+2A_{25}(W_2+W_3)\}$	$A_{23}U_3$
3	$A_{16}W_1$	$A_{23}U_1$	$A_{33}U_1+A_{66}V_1$	$A_{16}W_2$	$A_{23}U_2$	$\frac{1}{2}\{A_{33}(U_2+U_3)$ $+A_{66}(V_2+V_3)\}$
4	$\frac{1}{2}A_{11}(U_2+U_3)$	$A_{12}U_2+A_{15}W_1$	$A_{16}W_2$	$A_{11}U_4$	$A_{12}U_4+A_{15}W_4$	$A_{16}W_4$
5	$A_{12}U_3+A_{15}W_3$	$\frac{1}{2}\{A_{22}(U_2+U_3)$ $+A_{55}(V_2+V_3)$ $+2A_{25}(W_2+W_3)\}$	$A_{23}U_2$	$A_{12}U_4+A_{15}W_4$	$A_{22}U_4+A_{55}V_4+2A_{25}W_4$	$A_{23}U_4$
6	$A_{16}W_3$	$A_{23}U_3$	$\frac{1}{2}\{A_{33}(U_2+U_3)$ $+A_{66}(V_2+V_3)\}$	$A_{16}W_4$	$A_{23}U_4$	$A_{33}U_4+A_{66}V_4$

$A_{11} = \frac{1}{r}(k^2r^2+m^2)$, $A_{22} = \frac{1}{r}(k^2r^2+1)$, $A_{33} = \frac{1}{r}m^2$,

$A_{55} = r$, $A_{66} = r$, $A_{23} = -mk$,

$A_{25} = 1$, $A_{16} = -kr$, $A_{12} = -\frac{m}{r}$,

$A_{15} = -m$,

U_μ, V_μ and W_μ ($\mu = 1, 2, 3, 4$) are given in Table 1.

Table 4 Eight different modes of the instability classified from the viewpoint of the symmetry consideration.

	X	U	Z
Mode I	$X_e \cos n\varphi$	$U_o \cos n\varphi$	$Z_o \cos n\varphi$
Mode II	$X_o \sin n\varphi$	$U_e \sin n\varphi$	$Z_e \sin n\varphi$
Mode III	$X_e \cos n\varphi$	$U_o \cos n\varphi$	$Z_e \sin n\varphi$
Mode IV	$X_o \sin n\varphi$	$U_e \sin n\varphi$	$Z_o \cos n\varphi$
Mode V	$X_e \cos n\varphi$	$U_e \sin n\varphi$	$Z_o \cos n\varphi$
Mode VI	$X_o \sin n\varphi$	$U_o \cos n\varphi$	$Z_e \sin n\varphi$
Mode VII	$X_e \cos n\varphi$	$U_e \sin n\varphi$	$Z_e \sin n\varphi$
Mode VIII	$X_o \sin n\varphi$	$U_o \cos n\varphi$	$Z_o \cos n\varphi$

Table 5 Matrix elements used for the analysis of a toroidal plasma which is corresponding to the matrix (C_i) of the one-dimensional case.

$$a^N = \begin{pmatrix}
b(i,i,f), & c(i,i,fg), & c(i,i,hf), & d(i,i,f), & e(i,i,fg) & e(j,i,hf), & d(i,k,f) & e(i,k,fg), & e(k,i,hf) \\
--- & b(i,i,g), & c(i,i,gh), & e(j,i,fg), & d(i,j,g) & e(i,j,gh), & e(k,i,fg), & d(i,k,g), & e(i,k,gh) \\
--- & --- & b(i,i,h), & e(i,j,hf), & e(i,j,gh), & d(i,j,h), & e(i,k,hf), & e(k,i,gh), & d(i,k,h) \\
--- & --- & --- & b(j,j,f), & c(j,j,fg), & c(j,j,hf), & d(j,k,f), & e(j,k,fg), & e(k,j,hf) \\
--- & --- & --- & --- & b(j,j,g), & c(j,j,gh), & e(k,j,fg), & d(j,k,g), & e(j,k,gh) \\
--- & --- & --- & --- & --- & b(j,j,h), & e(j,k,hf), & e(kmj,gh), & d(j,k,h) \\
--- & --- & --- & --- & --- & --- & b(k,k,f), & c(k,k,fg), & c(k,k,hf) \\
--- & --- & --- & --- & --- & --- & --- & b(k,k,g), & c(k,k,gh) \\
--- & --- & --- & --- & --- & --- & --- & --- & b(k,k,h)
\end{pmatrix}$$

$$a^N_{mn} = a^N_{nm}$$

$$b(I,I,F) = F_{11}\alpha_I^2 + F_{22}\beta_I^2 + F_{33}\gamma_I^2 + 2F_{12}\alpha_I\beta_I + 2F_{13}\alpha_I\beta_I ,$$

$$c(I,I,F) = F_{11}\alpha_I^2 + (F_{12} + F_{21})\alpha_I\beta_I + (F_{31} + F_{13})\alpha_I\gamma_I,$$

$$d(I,J,F) = F_{11}\alpha_I\alpha_J + F_{22}\beta_I\beta_J + F_{33}\gamma_I\gamma_J + F_{12}(\alpha_I\beta_J + \alpha_J\beta_I) + F_{13}(\alpha_I\gamma_J + \alpha_J\gamma_I)$$

$$e(I,J,F) = F_{11}\alpha_I\alpha_J + F_{12}\alpha_I\beta_J + F_{21}\alpha_J\beta_I + F_{31}\gamma_I\alpha_J + F_{13}\gamma_J\alpha_I + F_{23}\beta_I\gamma_J + F_{32}\beta_J\gamma_I,$$

$$f_{11} = \beta_{11} = \left(\frac{n\mu}{RJB}\right)^2 + \left(\frac{\mu' R}{J}\right)^2 + \gamma P\left(\frac{J'}{J}\right)^2 + \frac{J'P'}{J} + \frac{I'\mu}{J},$$

$$f_{22} = \beta_{44} = B^2 + \gamma P\left(\frac{B\mu}{J}\right)^2,$$

$$f_{33} = \beta_{77} = (RJB)^{-2},$$

$$f_{12} = \beta_{14} = \mu\mu'\left(\frac{R}{J}\right)^2 + \frac{\gamma PJ'}{J} + \frac{P'}{2} - \frac{\mu I'}{2J} - \frac{j}{2R},$$

$$f_{13} = \beta_{17} = 0,$$

$$fg_{11} = \beta_{12} = \frac{\gamma nPJ'}{J} + \frac{P'n}{2} - \frac{n\mu I'}{2J} - \frac{nj}{2R},$$

$$fg_{12} = \beta_{15} = 0,$$

$$fg_{13} = \beta_{18} = \frac{I'}{2J} - \frac{R^2}{J^2}\mu',$$

$$fg_{21} = \beta_{42} = nB^2 + \gamma nP,$$

$$fg_{31} = \beta_{73} = -\frac{I'}{2J},$$

$$fg_{23} = \beta_{48} = -\frac{\mu R^2}{J^2},$$

$$fg_{32} = \beta_{75} = 0,$$

$$g_{11} = \beta_{22} = n^2B^2 + \gamma Pn^2,$$

$$g_{22} = \beta_{55} = 0,$$

$$g_{33} = \beta_{88} = \left(\frac{R}{J}\right)^2,$$

$$g_{12} = \beta_{25} = 0,$$

$$g_{13} = \beta_{28} = 0,$$

$$gh_{11} = \beta_{23} = \frac{\gamma n^2 P\mu}{J},$$

$$gh_{12} = \beta_{26} = 0,$$

$$gh_{13} = \beta_{29} = \frac{\gamma nP}{J},$$

$$gh_{21} = \beta_{53} = 0,$$

$$gh_{31} = \beta_{84} = 0,$$

$$gh_{23} = \beta_{59} = 0,$$

$$hg_{32} = \beta_{86} = 0,$$

$$h_{11} = \beta_{33} = \frac{\gamma P}{J^2} n^2\mu^2,$$

$$h_{22} = \beta_{66} = 0,$$

$$h_{33} = \beta_{99} = \frac{\gamma P}{J^2},$$

$$h_{12} = \beta_{36} = 0,$$

$$h_{13} = \beta_{39} = 0,$$

$$hf_{11} = \beta_{31} = \frac{\gamma nP\mu J'}{J^2} + \frac{n\mu P'}{J},$$

$$hf_{12} = \beta_{34} = \frac{\gamma nP\mu}{J},$$

$$hf_{13} = \beta_{37} = \frac{P'}{2J},$$

$$hf_{21} = \beta_{61} = 0,$$

$$hf_{31} = \beta_{91} = \frac{\gamma PJ'}{J^2} + \frac{P'}{2J},$$

$$hf_{23} = \beta_{67} = 0,$$

$$hf_{32} = \beta_{94} = \frac{\gamma P}{J},$$

$\beta_{ik} = \beta_{ki}$, $\beta_{44} = \beta_{45} = \beta_{46} = \beta_{47} = \beta_{55} = \beta_{56} = \beta_{58} = \beta_{66} = \beta_{69} = \beta_{77} = \beta_{78} = \beta_{79} = \beta_{88} = \beta_{89} = \beta_{99} = 0$,

but for Mode-I and II, $fg_{11} = hf_{11} = fg_{21} = gh_{13} = hf_{12} = 0$, for Mode III and IV, $fg_{11} = hf_{31} = gh_{11} = fg_{21}$ $= hf_{13} = fg_{32} = 0$, for Mode-V and VI, $hf_{11} = fg_{13} = gh_{11} = fg_{31} = hf_{12} = fg_{23} = 0$ and for Mode VII and VIII, $fg_{13} = hf_{31} = fg_{31} = gh_{13} = hf_{13} = fg_{23} = hf_{32} = 0$.

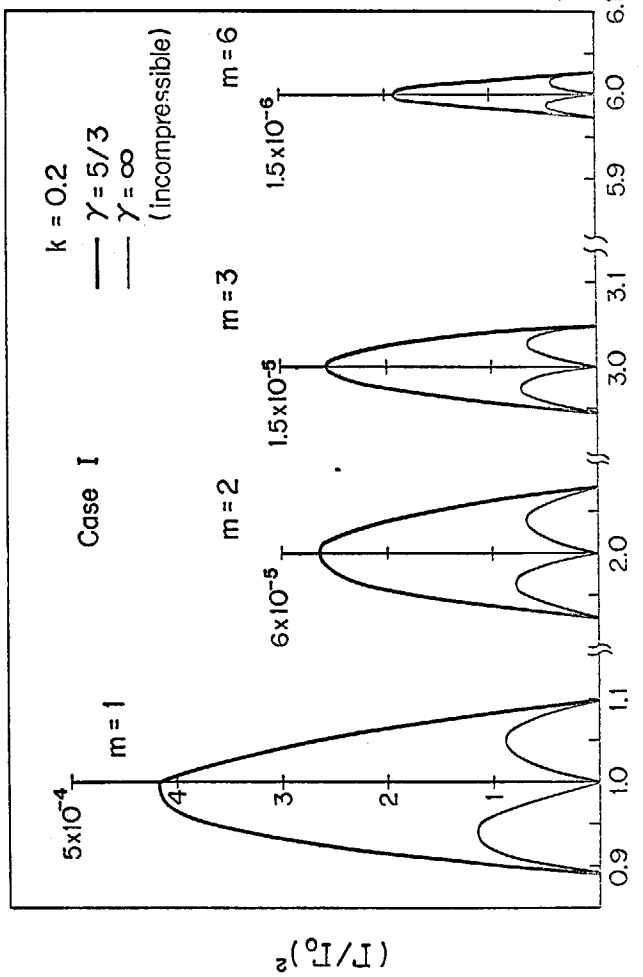

Fig. 2 Growth rates of various modes with fixed boundary. The bold and the thin lines show the growth rate for the compressible plasma ($\gamma=5/3$) and the incompressible plasma ($\gamma=\infty$), respectively.

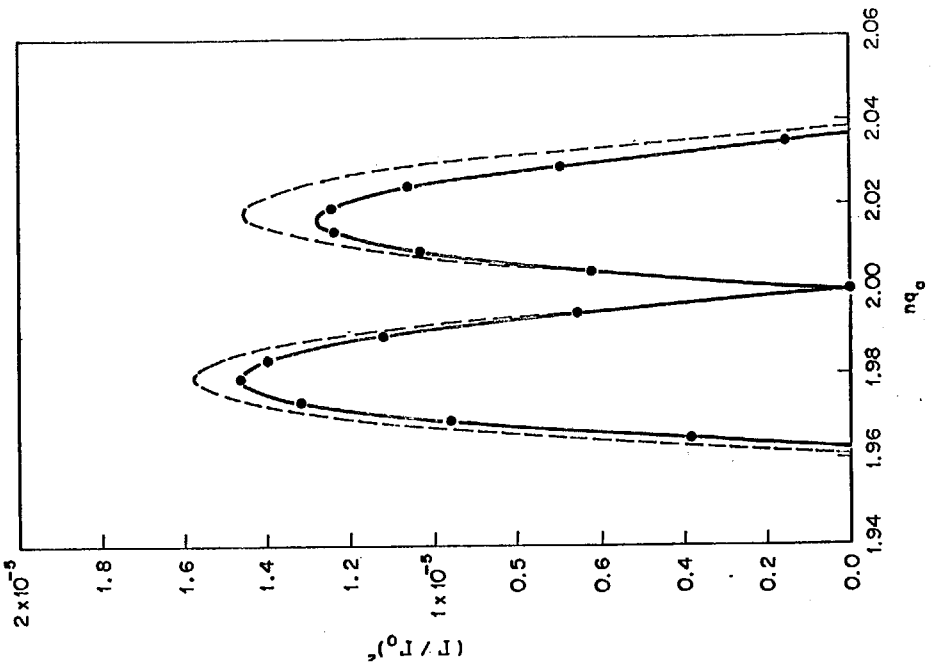

Fig. 1 Growth rate of the m=2 mode for an incompressible plasma with a fixed boundary. The solid and the broken lines show the numerical and the analytical result[5], respectively.

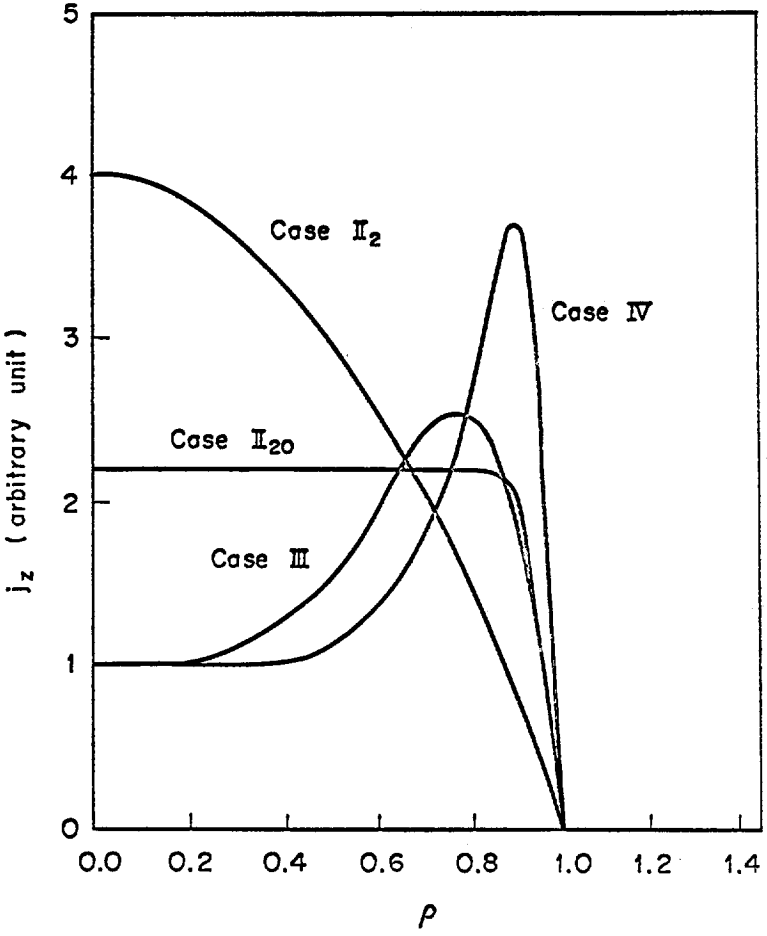

Fig. 3 Various current distributions used in the numerical calculations. The cases II_2 and II_{20} correspond to the current distribution of s=2, $j_0=j_2=0$ and s=20, $j_0=j_2=0$, respectively. The cases III and IV correspond to the current distribution of s=20, t=4 and s=20, t=10, respectively, where $j=(s+2)/(2s)$ and $j=\frac{1}{4}(t+2)(t+3)$.

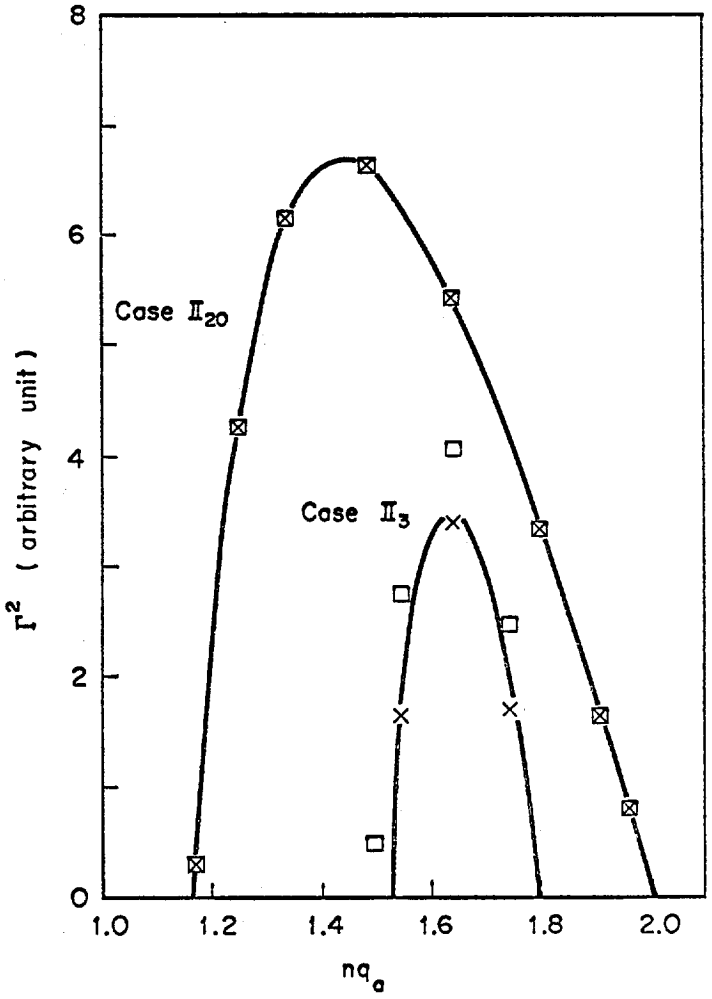

Fig. 4 Dependence of the convergence of the numerical method on the number of meshes and the current distributions, for m=2 mode (the free boundary case). The solid line indicates the numerical result for the case of $N_0=10$, $N_1=3$. □ and × indicate the results for the cases of $N_0=20$, $N_1=3$ and $N_0=5$, $N_1=3$, respectively.

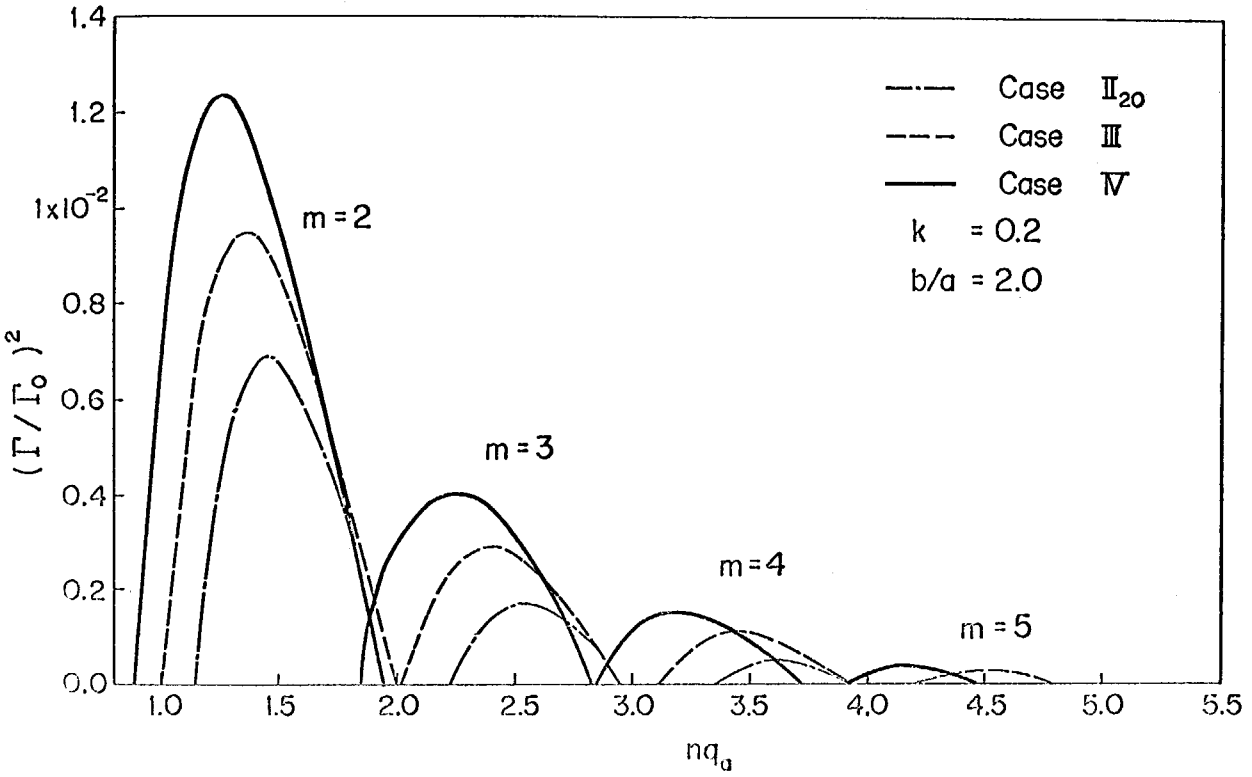

Fig. 5 Growth rates of various modes of free boundary case.

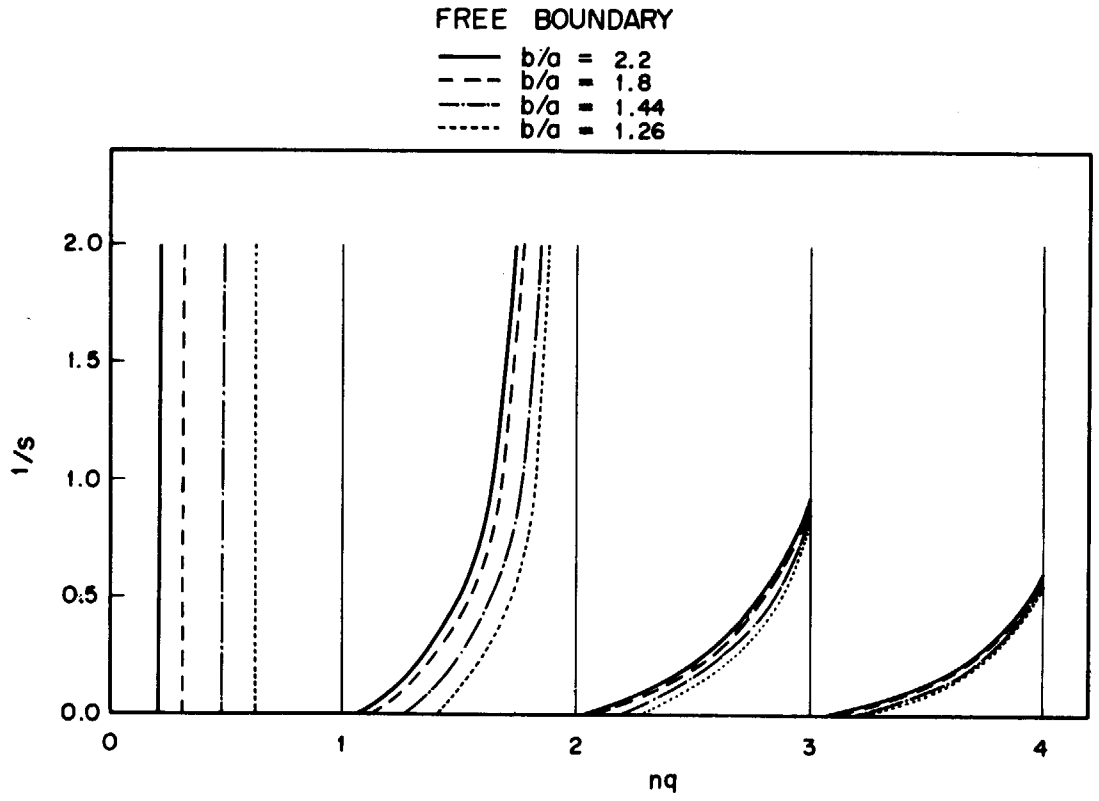

Fig. 6 Unstable regions in the nq-1/s plane. Shaded are the unstable regions for m=1, 2, 3 and 4 modes where b/a=1.43.

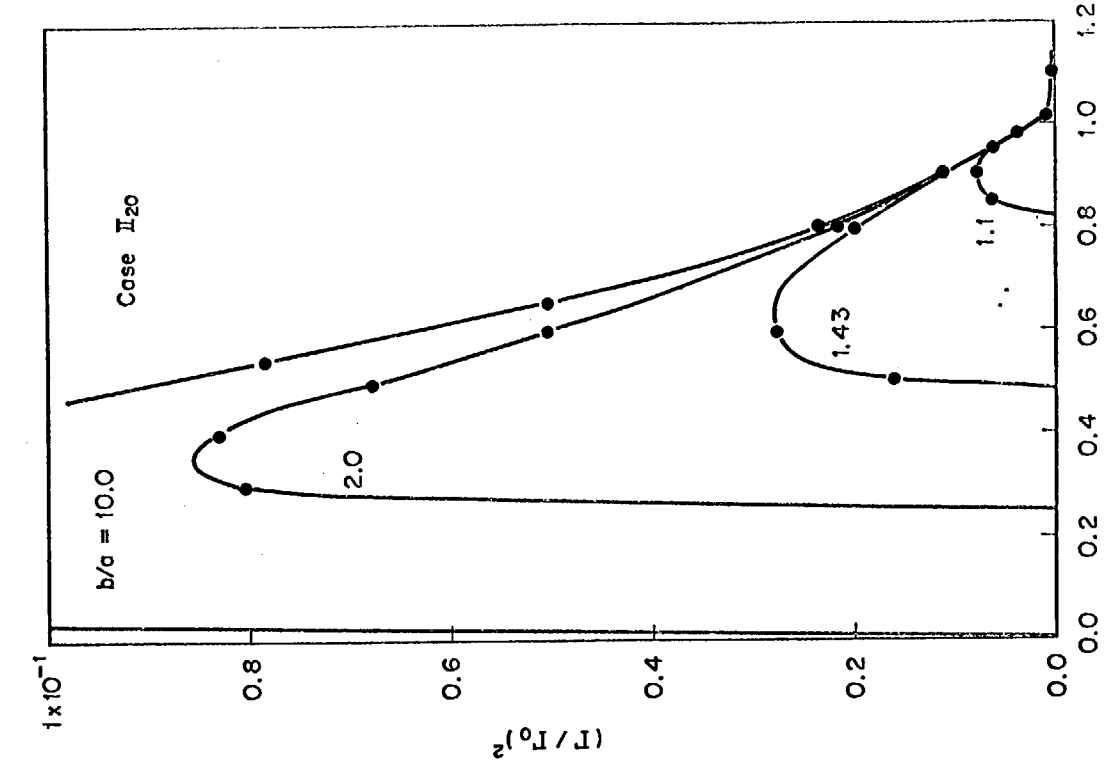

Fig. 8 Dependence of the growth rate on the positions of the conducting wall for the m=1 mode.

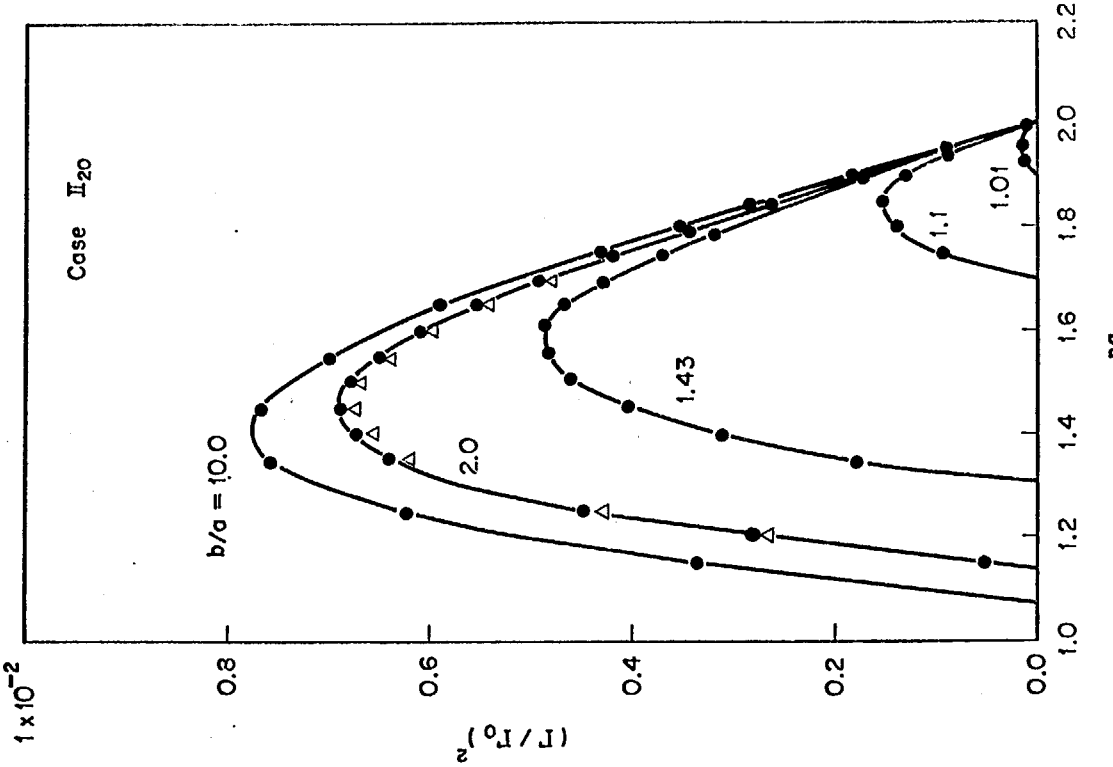

Fig. 7 Dependence of the growth rates on the ratio of specific heat and the positions of the conducting wall. The circles indicate the cases of $\gamma = 5/3$ and the triangles indicate the cases of $\gamma = 5/3 \times 1000$.

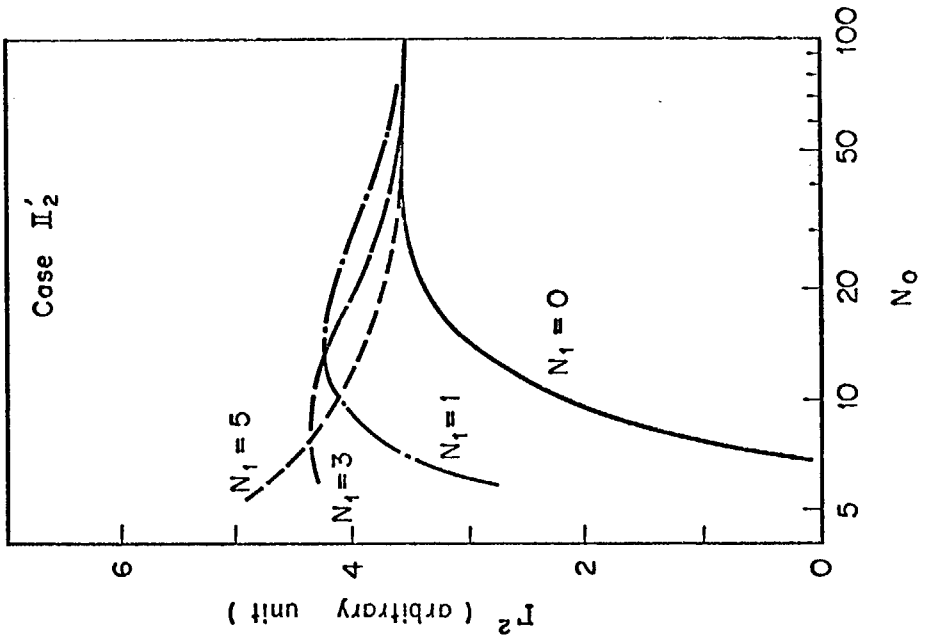

Fig. 10 Dependence of the growth rate on the number of meshes. The calculations are carried out for the m=2 mode with b/a=1.43 and q_a=1.725.

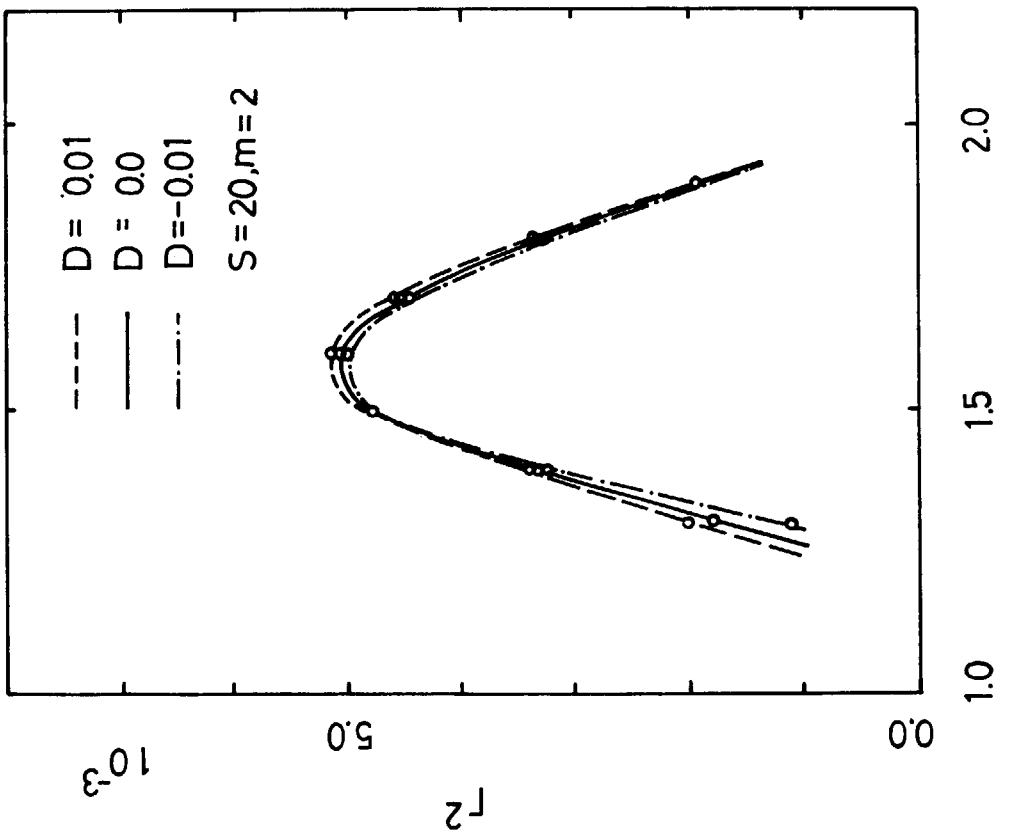

Fig. 9 Dependence of the growth rate on the distribution of the longitudinal magnetic field, for m=2, s=20 and b/a=1.43.

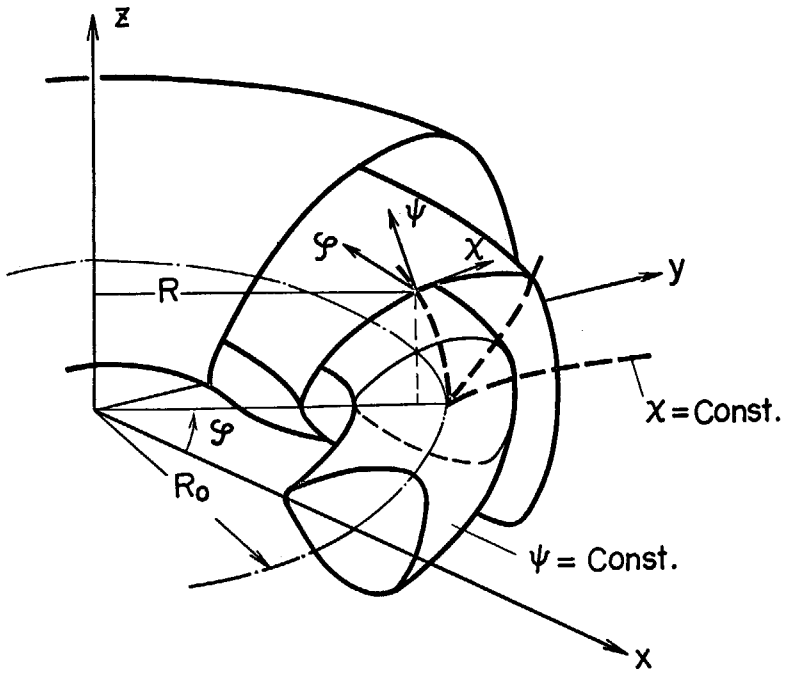

Fig. 11 Coordinate system for the analysis of an axi-symmetric toroidal plasma.

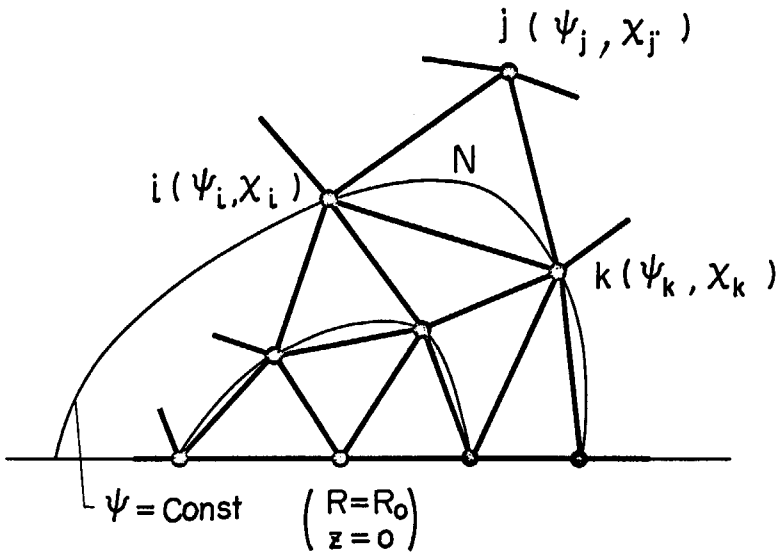

Fig. 12 Schematic diagram of meshes for the analysis of an axi-symmetric toroidal plasma.